University of Stavanger

Faculty of Science and Technology

MASTER THESIS

Study program/Specialization: MSc Petroleum Geosciences Engineering	Spring semester, 2016 Open / Restricted access
Writer: Fikri yunus	…… (Writer's signature)
Faculty supervisor: Christopher Townsend, University of Stavanger External supervisor: Lothar Schulte, Schlumberger	
Thesis title: Facies Modelling Based on Multi-Point Statistics (MPS) in Submarine Fan Deposits	
Credits (ECTS): 30	
Key words: Multi-point statistics (MPS) Multi-point facies simulation (MPFS) Training Image Submarine fan deposits	Pages: 69 + enclosure: …… Stavanger, 15th June 2016

Copyright

by

Fikri Yunus

2016

Facies Modelling Based on Multi-Point Statistics (MPS) in Submarine Fan Deposits

BY

Fikri Yunus

THESIS

Presented to the Faculty of Science and Technology

The University of Stavanger

THE UNIVERSITY OF STAVANGER

JUNE 2016

ACKNOWLEDGEMENTS

There are so many wonderful people to thank for helping me during the last two year. So many have made my short stay in Stavanger a lot easier than I thought it was going to be.

First, I would like to thank my supervisor **Lothar Schulte** for his guidance, encouragement, support and patience over the last nine months. Thank you so much for forcing me, sometimes kicking, to look at research and my work in different ways and for opening my mind. Your support was essential to my success. I would also thank **Christopher Townsend** as my internal supervisor, especially for giving me a seat in the Stat Oil Lab.

Felicia Ratna Hapsari has been willing to be engaged in my struggle to write this thesis. A very special thank you for your practical and emotional support.

Of course, I would like to thank all my classmates: Sindre, Espen, Muddassar, Darjan, Erik, Hans, Stian, Bilal, Prateek, Victoria, Lena, Ine, Camilla Hinna, Ekaterina, Biswarup, Javed, Thanh, Yichen, Diana, Rosita, Camilla Sæther, Silje, Mohammed and Jinx, for spending a lot of time together and also for the never ending discussion.

ABSTRACT

Facies Modelling Based on Multi-Point Statistics (MPS) in Submarine Fan Deposits

Fikri Yunus

University of Stavanger, 2016

Supervisors: Christopher Townsend & Lothar Schulte

Multi-point statistics (MPS) is a relative new geostatistical facies modelling technique that was welcomed by oil industry as a promising alternative to the classical methods (object-based and pixel-based modelling). However today, this method is yet not widely used by geo-modeller. This thesis is a conceptual study focusing on the development of methodologies and best practices for MPS application to submarine fan deposits. For the conceptual study, 6 wells are available. The facies logs are re-interpreted following published work of turbidite systems. Based on analogue data, a conceptual model is created that integrates the available well data. Training images that are used as the main driver of MPS can be regarded as the link between the conceptual model and the facies simulation. One serious limitation of training images is the request of stationary, because this can be in conflict with complex depositional environments such as turbidite systems. However this limitation has been avoided in this study thru subdividing the conceptual model into several regions and assigning to each region a different training image. The vertical dimension of the turbidites of the training images is derived from analogue data that delivers the relationship between the submarine channel width and the channel depth. Vertical and horizontal gradual changes of the facies are addressed thru setting up probability distributions.

Based on the conceptual model, six facies models are carried out using different methods. Four methods are based on multi-point statistics (MPS) using different groups of training images: single layer training images of two facies, multilayer training images of two facies, multilayer training images of three facies and multilayer object modelling training images. Two additional methods are carried out using Gauss indicator simulation (GIS) and object modelling. Based on the experience gained by this study best practices are given.

TABLE OF CONTENTS

LIST OF TABLES

LIST OF FIGURES

1. INTRODUCTION

Submarine fan deposits are attractive reservoir targets for the oil industry. However these reservoirs are generally challenging to be developed. For instance one of the challenges is to reduce the risk and the cost of the field development scenario. Typically, these challenges are addressed thru building of numerical reservoir models for hydrocarbon volume estimation, uncertainty consideration, flow simulations and well placement.

The idea of reservoir modelling is to combine the petrophysical data from well logs with the seismic data. Well data have a high resolution of ca 0.2 m but are sparsely distributed while the seismic data is laterally densely sampled and covers a large area but has a low vertical resolution of 15-40 m. Therefore, a conceptual model, which is the underpinning of reservoir modelling, is created based on the interpretation of the well logs, the seismic data as well as analog data and geological background knowledge.

In general, reservoir modelling uses a geostatistical approach for the spatial distribution of the facies and petrophysical properties. The geostatistical modelling allows stochastic simulation of the reservoir properties that provides alternative, equi-probable, solutions that can be used for capturing the model uncertainty (Journel, 1994). The most common stochastic simulation techniques for facies modelling are object-based modelling, Gauss indicator simulation (GIS) using two-point statistics and the multi-point statistics (MPS) method that tries to capture the depositional environment thru training images.

Guardiano and Srivastava (1993) were the first who introduced MPS. Strebelle (2000) in the form of SNESIM (Single Normal Equation Simulation) developed the method further. However, MPS was not widely used by reservoir modelers at that time because of the limitation of computer technology. Today, rapidly evolving computational technology makes the MPS a valid alternative for facies modelling.

Facies modelling based on MPS is also called multi-point facies simulation (MPF)S and is regarded as a promising tool to model complex geological architectures as seen in modern analog data or outcrops. An important characteristics of MPFS is that it honors the well log data (hard

data) and allows to condition the facies simulations thru probability cubes, seismic attributes or geometrical scaling. These properties make MPFS a flexible facies modelling method.

Tetzlaff et al. (2005) use a deepwater outcrop analog of the Tanqua Karoo Basin, South Africa to create the facies model using MPFS. The input data are 350 outcrop logs and 6 cored and wireline-logged boreholes. The single layered training images have complex patterns consisting of up to five facies. The final model shows the MPFS that honors the well data, the rotational and the affinity fields, and soft probabilities.

Strebelle, Payrazyan, and Caers (2003) are using the MPFS method to create a facies model of a deepwater turbidite reservoir. They build a prior geological model as the training image. The training image is single layered and has two facies, sand and not-sand. As additional input, facies probabilities are derived from seismic amplitudes. The results show how MPFS is utilizing the facies probabilities to constrain the connectivity of facies.

In contrast to the above results, Harris et al. (2011) use multilayer training images to simulate the heterogeneity of carbonate ramps of the subsurface. They use outcrop analogs, modern analogs, and stratigraphic models to get information of the size, shape and spatial relations of the facies. The training images show the progradational and retrogradational pattern with a simple facies relationship. In addition, they use a vertical proportion curve and facies probability cubes to guide the facies distribution. The result reveals how MPFS can capture the details of the facies architecture and heterogeneity shown by the outcrop analogs.

The main objective of this thesis is to develop methodologies and best practices for facies modelling of a submarine fan deposits by using MPFS for a submarine fan deposits. This conceptual study is using the data of six wells and published analog models of submarine fan reservoirs. The results of MPFS are compared with the facies models based on the classic modelling methods (Gauss indicator simulation (GIS) and object modelling).

Only few, if any, MPFS studies explain the usage of multilayer training images in a complex depositional environment such as submarine fans, estuary or delta. Therefore, the additional objective of this thesis is to investigate multilayer training images and their impact on the MPFS.

2. SUBMARINE FAN SYSTEM THEORY

2.1 Introduction

Submarine fans are bodies of sediment deposited by mass-flow processes. The sediments may have a fan-shaped or lobate geometry, which is controlled by the composition of the materials supplied that may have originated from the deltas or shelf deposits (Nichols, 2009).

The deposits have a complex reservoir architecture which is controlled by the slope gradient, the slope profile, the topography evolution, the type of delivery system and the common association with erosional bypass (Ravnås et al., 2014). Piper and Normark (2009) suggest the important mechanism to generate prolonged or sustained sediment turbidity flows by hyperpycnal flows which are generated from rivers in flooding events.

Turbidity currents are driven by gravity containing opaque mixtures of sediments and water (turbid), which may contain gravel, sand and mud, temporarily suspended in water. These flows can occur anywhere where there is a supply of sediment and a slope. The deposition mechanism that is initially suspension in the turbidity currents may come to a halt or move on by rolling or suspension when approaching the deep marine surface.

2.2 Architecture Element

The architecture elements of a submarine fan consist of channels and levees in the proximal fan, depositional lobes in the medial fan, and turbidite sheets in the distal fan surrounded by a basin plain (Figure 2-1). A channel is deposited via the mechanism of high to medium density of turbidite systems. The levee is a product of over-spill by the channel which is analogous to the overbank deposits of fluvial systems. Submarine fan channels that might scour into underlying submarine fan deposits are of varying size, and may have a width of up to tens of kilometers. Typically, the channel sediments consist of coarse sand and gravel that form thick, structure-less or crudely graded beds. The levee deposits can build up to several hundred meter of thickness corresponding to the channel aggradation.

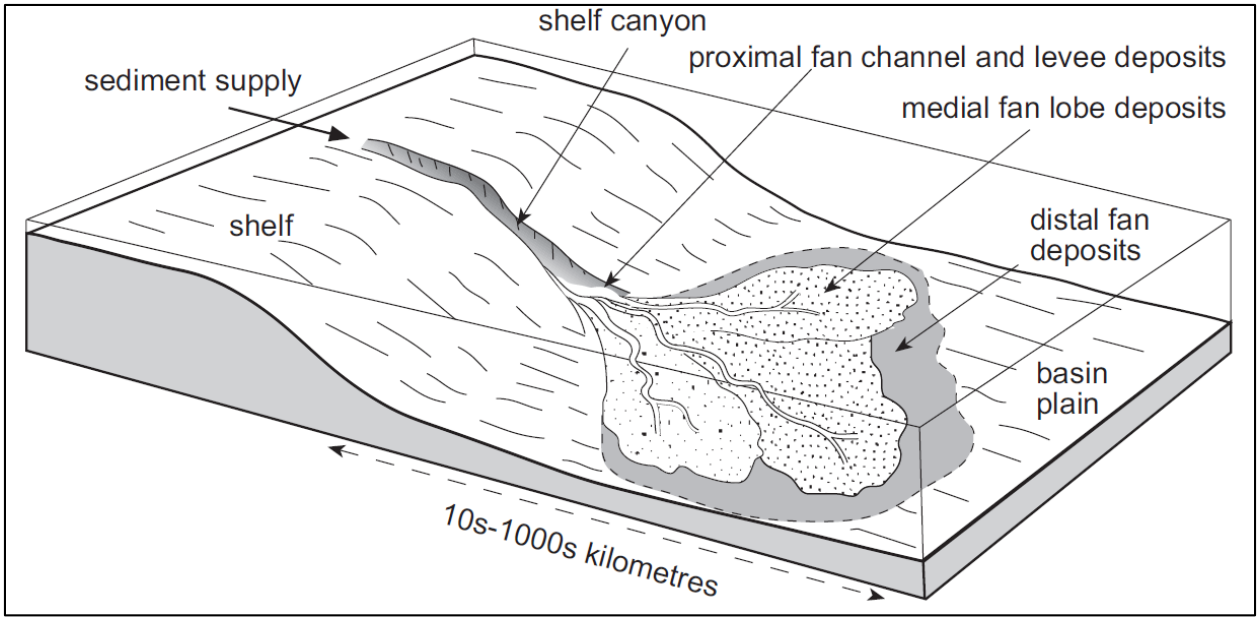

Figure 2-1 Submarine fan architecture elements (Nichols, 2009)

Depositional lobes are part of the medial fan where turbidity currents spread out to form lobe deposits. The turbidity currents tend to deliver the sedimentation further and further out to construct individual lobes. These currents have the same magnitude depositing progressively further from the mouth of the channel to form a simple progradational geometry of lobe. The progradational trend continues until the channel avulses following slightly steeper gradient into lower part of the fan. The depositions may have a thickness of several hundred meters, and a width of tens of kilometers.

At the outer part of the depositional lobe, the turbidite current spreads out over a larger area of the fan and deposits fine sand. These deposits have a fine-grained lithology, and show thin interbedding with hemipelagic mudstones.

2.3 Submarine Fan Systems Classification

Reading and Richards (1994) classify submarine fan systems based on the source and the grain size of the sediment material. Based on the grain size, submarine fan deposits can be divided into mud-rich systems, mud/sand rich systems, sand-rich systems and gravel-rich systems where each system has a different sand shale ratio.

A mud-rich system is characterized by its large size (radius range from 100 km up to 3000 km) and elongated shape. Thus, this system is covering large areas with a large volume of sediments,

far traveling distance, and low-density turbidity currents. The modern analogue of this system is the Mississippi Fan supplied by large deltas through large fan valleys. The sand-shale ratio of this system is less than 30%. The sand-shale ratio along the main channel axis is largest because the majority of sand sediments deposit in the channel-levee system.

A mud/sand-rich system is of moderate size with a radius between 10 and 450 km, and the shape is lobate rather than elongate. The sediment source comes from a moderate sized mixed-load delta, beach, or shoreface deposits cut by the canyon. The feeder channel in the upper part of the fan contains sands that are linked shoreward with a shoreline, shelf, or deltaic sands. The main channel is divided into distributaries that aggrade to form supra-fan bulge in the upper middle fan. Concerning the lower fan, the channel deposits over prograding lobes during periodic of avulsions. The hemipelagic mudstones predominate over the deposits in the lower fan and basin plain because of the low magnitude of the turbidity currents. In this system, the percentage of sands ranges from 30 to 70%. Increasing the sand content leads to channel switching or migration due to a decrease in levee stability.

A sand-rich system shows dominance of sand and is moderate in size with a radius between 5 and 10 km, and is of radial shape. The size of the sand-rich submarine fans is smaller than the mud-rich or mud/sand-rich systems. The sediment supplies are from sand rich shelfs and coastal systems and carried into the basin via canyons. The volumes of sediment in this system depend on the size and tectonic of the basin where very large volumes of sediment deposit during sea level rises or highstands. The percentage of the sands in this system is more than 70%. A channelized lobe system lead to the formation of a low sinuosity to braided system of channels that switch constantly across the fan surface. The deposits show thick, massive, and aggrading-upward sandstones forming a suprafan.

The last category is the gravel-rich system. This system comprises of coarse-grained sediments covering an area with a radius between 1 and 5 km. The sedimentation processes include debris avalanching, inertia and turbidity flows, and various slope instability processes, while fine-grained sand, silt, and clay settle out from suspension. Storms, annual floods, or very high-magnitude events related for instance to glacier melting or tectonic activity affect directly and immediately the sedimentation process of gravel-rich systems. The coarse-grained lobes are fed by submarine channels (chutes) and slumps forming a debris flow. The feeder systems may be controlled by

transfer zones and other minor faults transverse to the basin axis. This system has a sand-shale ratio which ranges from 50 to 80%.

3. FACIES MODELLING THEORY

3.1 Multi-Point Statistics Facies Modelling Theory

3.1.1 Introduction

In 1998, sequential Gaussian simulation (SGS) and sequential indicator simulation (SIS) were developed by Deutsch and Journel that are widely used in stochastic reservoir modelling (Arpat, 2005). These techniques were originally setup to reproduce the data histogram and their distribution in space through simple kriging and the sequential random drawing from the conditional probability distribution function (cpdf) provided by the kriging result (Arpat & Caers, 2007). However, these algorithms cannot scope with complex geological structures because they are based on two-point correlations provided by the variogram model (Arpat & Caers, 2007; Zhang, 2009).

As an alternative to SGS and SIS, Guardiano and Srivastava (1993) proposed the concept of the training image. This idea was the starting point of the development of multiple-point statistics (MPS). Strebelle (2000) created fluvial channel reservoir models based on the MPS method which they called SNESIM (Single Normal Equation Simulation). This algorithm overcomes the serious performance limitation of the older MPS algorithms and therefore has been accepted as an alternative modelling tool.

3.1.2 Training Image

A training image is a simplified numerical representation of the geological subsurface, which is used as the main driver to conduct the facies model (Zhang, 2009). Training images are conceptual patterns that reflect the general aspects of the spatial facies distribution. MPS theory requests that the training images show only stationary features consisting of repetitive patterns that do not have any local accuracy. The training image provides the relative size and relationship of the bodies. The absolute size of the training image is defined by the resolution of the model that is using the training images.

Ideally, the training image should be set up in a multilayer grid to reflect the lateral distribution and the vertical aggradation pattern of the facies. The stacking pattern of the facies is provided by the well log interpretation or outcrop analogs while the lateral distribution of the facies is guided by the depositional model and eventually by seismic attributes.

3.1.3 Search Mask

The search mask is a small section of the 3D Grid model consisting of a set of neighboring pixels/voxels centered around one pixel/voxel. The search mask can be of ellipsoid or rectangular shape. The dimension of the search mask is defined by the training image: for instance, a single layer training image requests a single layer search mask (Figure 3-1).

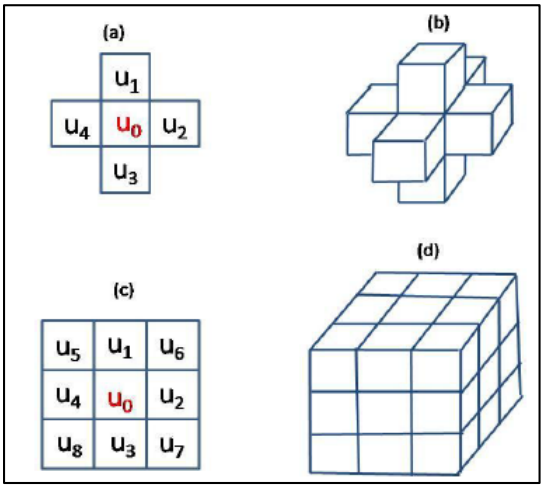

Figure 3-1 Examples of search mask (Zhang, 2009) a) A single layer ellipsoid search mask with 4 pixels in the search area b) Multilayer ellipsoid search mask with 6 voxels in the search area c) A single layer rectangular search mask has 8 pixels in the search area d) Multilayer rectangular search mask with 27 voxels.

3.1.4 MPS Principle

The principle of facies simulation based on MPS is discussed in Figure 3-2: In the simulation grid the grid cell labelled '*u*' (red pixel), whose facies shall be determined. This grid cell is located between two sand cells (black pixel) and two shale cells (white pixel). These four data values (sands and shales) are copied into the search mask. Scanning the training image with the search mask will find four replicates of the facies pattern of the mask. The center grid cell encounters three times sand and one times shale at these four mask grid positions. As shown in the small pictogram of Figure 3-2, this delivers the cumulative probability distribution function (cpdf) for the facies probability.

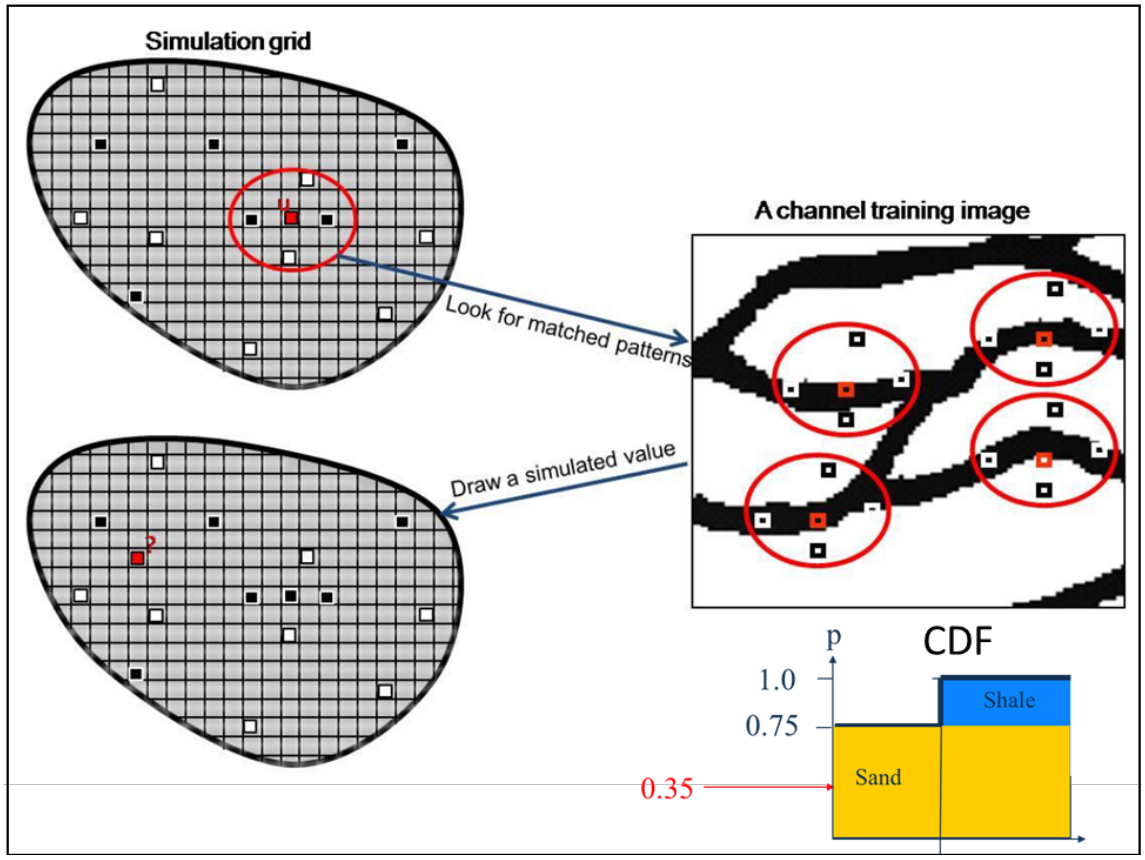

Figure 3-2 The illustration of the sequential facies simulation using Multi-Point Statistics (MPS) (Zhang, 2009).

The final step is similar to Gaussian indicator simulation (GIS). The grid cell to be simulated (u) gets the facies from the cpdf. With the help of a random number generator, a probability value is drawn (red number in the small pictogram of figure 3-2) and the corresponding facies taken from the cpdf. In this example, the random number is 0.35. Therefore, the sand facies (black pixel) is assigned to the grid cell u. The simulation is completed when the sequential process has visited all grid cells of the 3D model grid.

3.1.5 Physical Region

The physical region concept has the objective to simplify a complex reservoir thru subdividing it into several physical regions that have simple facies architectures. These physical regions can be derived from the concept of sub-environments of the depositional system or the facies association in specific areas of the reservoir. Each physical region has its own training image as an input as seen in Figure 3-3.

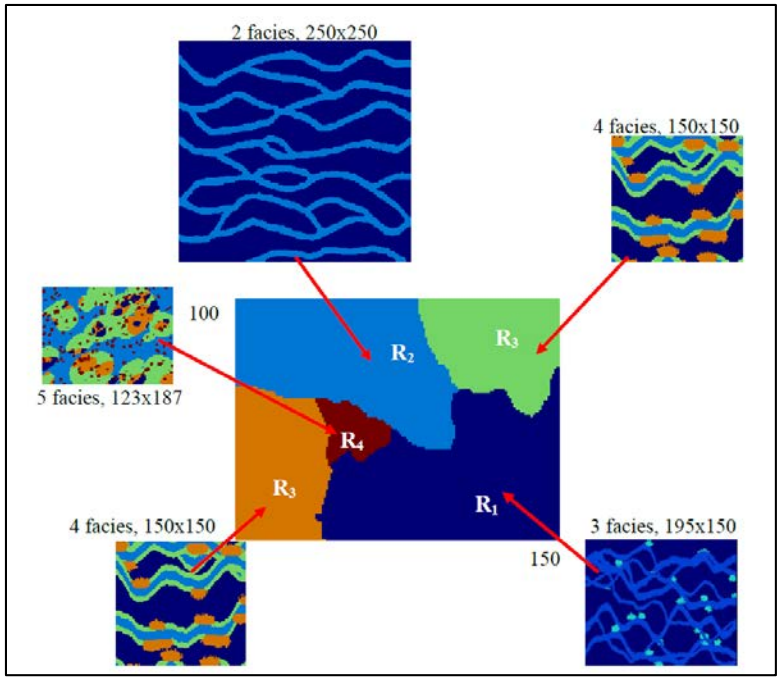

Figure 3-3 An example of simulation using the physical region concept with different training images (Zhang, 2009).

The simulation of each physical region is done sequentially (Figure 3-4). This means that the previously simulated physical region constrains the simulation of the following physical region. In this way the smooth transition across the boundary of physical regions is assured.

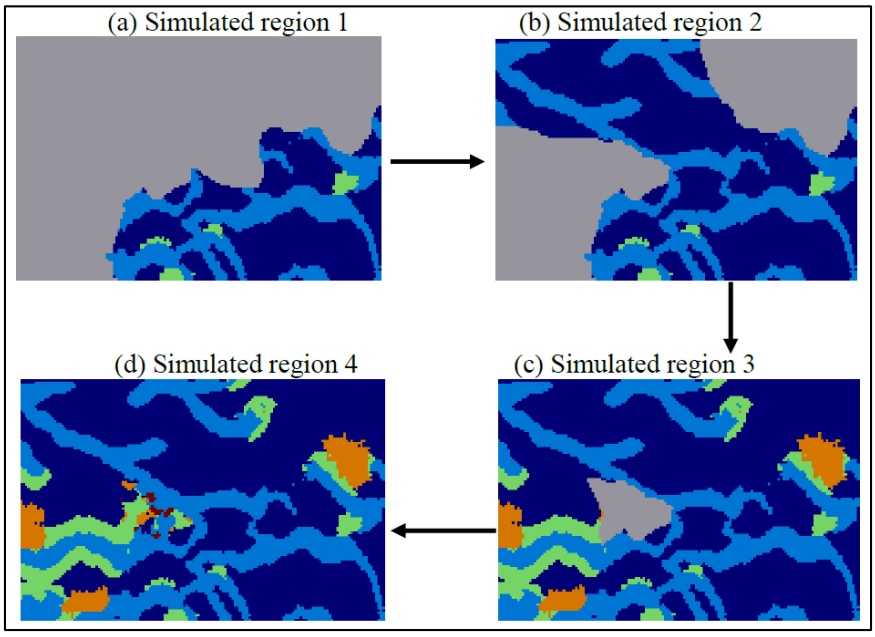

Figure 3-4 Simulation process using physical region concept (Zhang, 2009).

3.1.6 Azimuth and Scaling Factor

A depositional environment may have a depositional trend that is controlled by the paleo-topography. The depositional trend can be observed or interpreted from existing data. To model this trend, MPS uses an azimuth parameter as an input to steer the facies property. A scaling factor can be used to control the size of the facies geometry in the 3D grid. Both inputs can be provided as constant numbers, surface of 3D grid properties and applied independently to the X/Y/Z directions.

Figure 3-5 explains how the scaling factor is used in conjunction with the azimuth parameter to simulate non-stationary patterns in the facies model. The figure shows a conceptual model that is subdivided into several regions. Each region has its own local orientation and scaling parameter but uses the same training image. The scaling factor changes the size of the facies in the simulation grid relatively to the size of features in the original training image while the azimuth input is used to control the direction of the facies distribution.

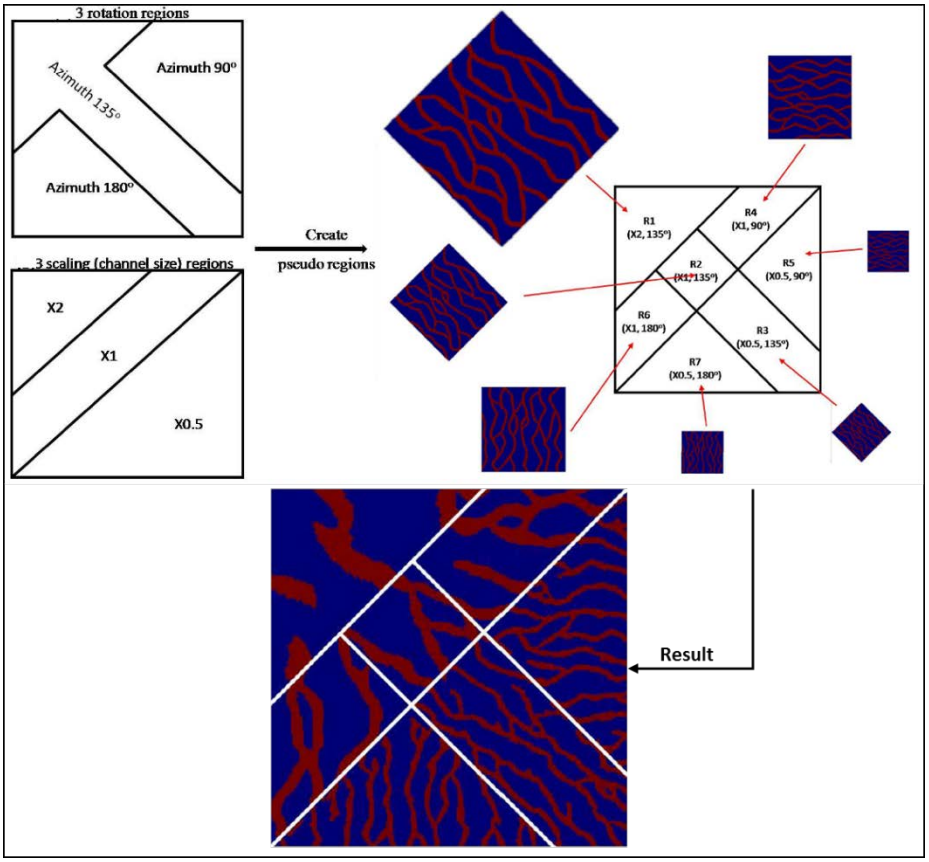

Figure 3-5 The illustration of using azimuth and scaling as additional inputs in MPS simulation (Zhang, 2009).

3.2 Pixel-Based Facies Modelling Theory

Gauss indicator simulation (GIS) is a method of pixel-based techniques. This method uses a variogram model as input to calculate the spatial distribution of the probability of each facies. The variogram is showing the spatial correlation between the probabilities of a specific facies given by the wells. The parameters of a variogram include variance, lag distance, sill, range, and nugget. The variance is a measure of how different members of a collection of data pairs are from each other for a specific lag distance. The lag distance, where the variance flattens and starts scattering around a mean value, the so-called sill, is the variogram range. The nugget measures the uncertainty of the data that results either from the lack of data for small separation distances or from measurement errors of the data.

The principle of GIS is illustrated in Figure 3-6. Each circle represents a facies measured at a well. A yellow circle means ‘sand’, a blue circle means ‘shale’ (Figure 3-6a). The numbers at the circles give the probability of encountering sand at the wells. As the facies at the wells are known, the sand probability at each well is either ‘1’ or ‘0’ depending whether sand or shale is encountered. The two blue crosses represent grid cells with already calculated sand probability. The sand probability at the grid cell highlighted by the red circle shall be calculated. First, the variogram is calculated for the sand probability given at the wells and grid cells with already derived sand probabilities (Figure 3-6b). The variogram model given by the red line in Figure 3-6b approximates the sample variogram. By using this variogram model as input, kriging is applied to calculate the sand probability of the grid cell highlighted by the red circle. In a similar way, the shale probability is calculated. From the two probabilities a cumulative probability distribution function (cpdf) is set up (Figure 3-6c). By using a random number generator, a random value between zero and one is drawn (red number in the Figure 3-6c) and the corresponding facies taken from the cpdf. In this example, the grid cell under consideration is assigned as shale facies. This sequential process is continue until all cells are visited.

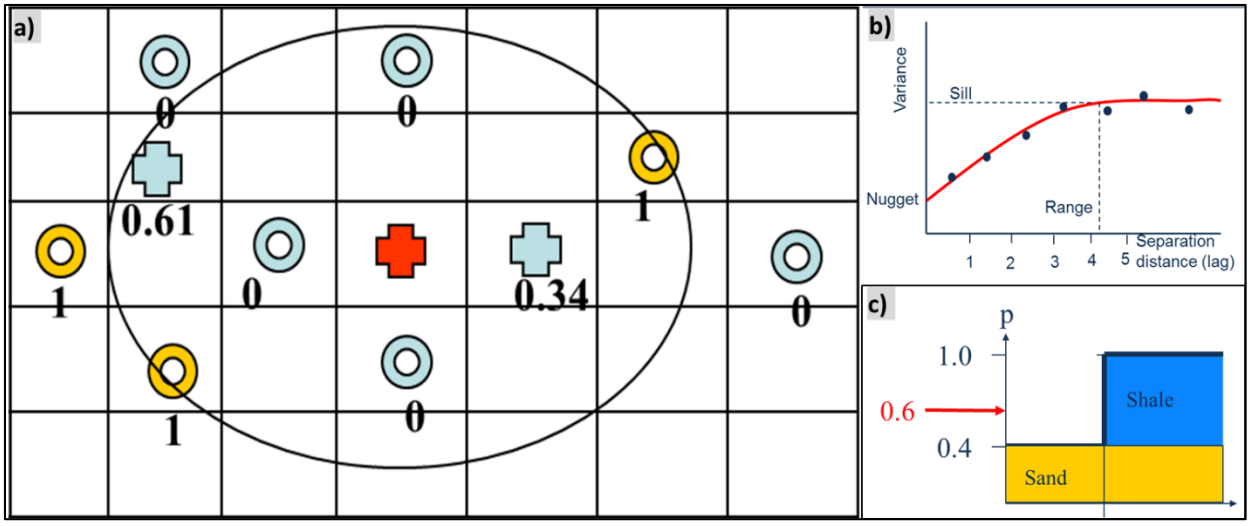

Figure 3-6 The illustration of Gauss indicator simulation a) The simulation grid b) The variogram c) The cumulative probability distribution function (cpdf).

3.3 Object-Based Facies Modelling Theory

Object-based modelling is a stochastic modelling technique where the geometry of the selected object is controlled by using specific parameters as input. The facies body can be either fluvial, fan lobe, oxbow lake, aeolian sand dune, or a simple geometrical body like half pipe, box, ellipse, etc.

The fluvial channel is a common object-based modelling algorithm that can be combined with levees and/or other objects. The parameters that need to be defined for controlling the body geometry are orientation, amplitude, wavelength, channel width, channel thickness as shown in Figure 3-7a. The fan lobe is controlled by the parameters, for example orientation, major width, minor width, lobe thickness and tapering (elongated shape) as seen in Figure 3-7b.

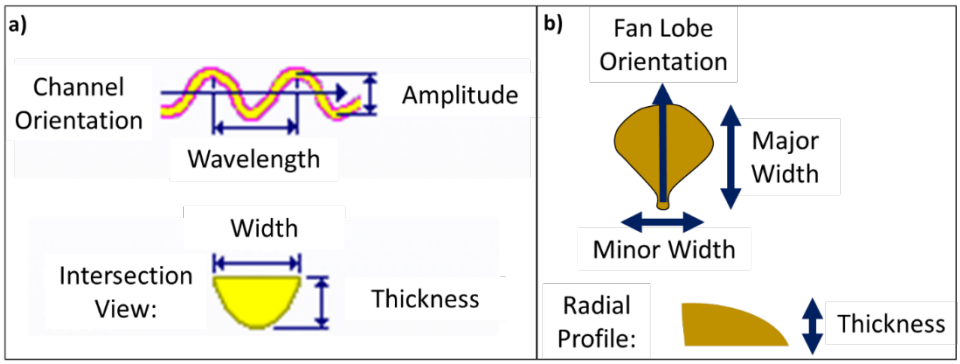

Figure 3-7 Examples of object parameters a) fluvial channel object parameters b) fan lobe object parameters.

4. METHODOLOGY

4.1 Introduction

This chapter starts with a description of the method used for setting up the facies logs of the six wells. Then the facies modelling processes using the multi-point facies simulation (MPFS) based on multi-point statistics (MPS) and the classical methods (pixel-based simulation and object-based simulation) are explained. In MPFS, four methods based on different types of training images are executed. The training images involved are: single layer training images of two facies, multilayer training images of two facies, multilayer training images of three facies, and multilayer object modelling training images. The pixel-based facies simulation is based on the Gauss indicator simulation (GIS) technique, and object-based facies simulation is using the object modelling technique. Finally, a connectivity analysis is conducted in order to compare the six methods.

4.2 Data Set Interpretation

Submarine fan deposits have a quite complex architecture from distal to proximal and central to marginal that can be observed at the six well data. Based on the grain size and the process of their formation, the facies of these deposits can be divided into channel-sand, lobe-sand, sheet-sand, and background-shale facies guided by the gamma ray log interpretation from literatures (Figure 4-1).

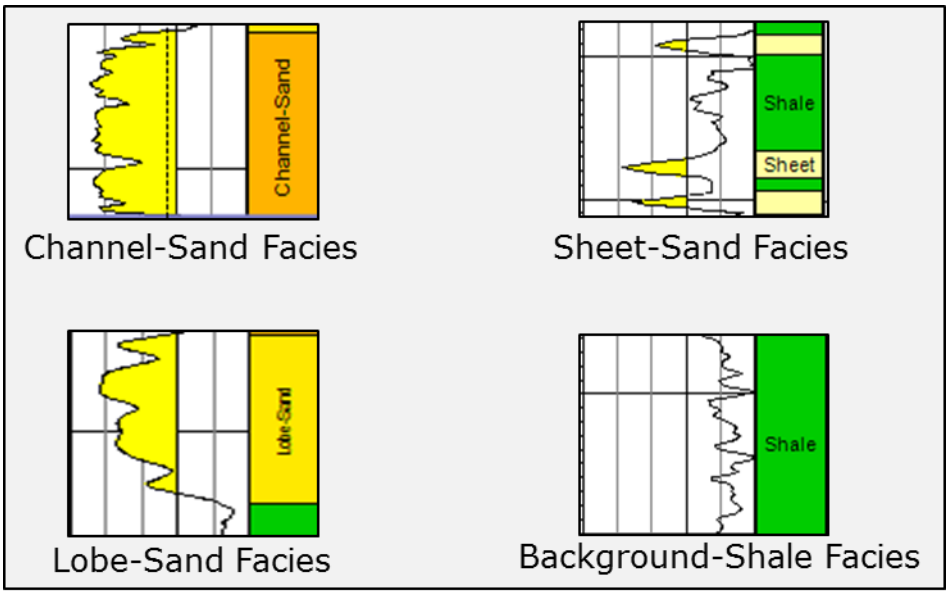

Figure 4-1 The facies log interpretation based on gamma ray log respond.

The individual channels created by turbidity flow can be analogized by channels of fluvial systems. This process deposits the channel-sand facies as channel fill. The thicker channel-sand units are a product of stacked amalgamated beds that can be observed in the well log data where the gamma ray log has a blocky shape and low values. The lower part of these deposits form a sharp erosive base indicating flow erosion.

Lobe-sand facies deposit at the distal ends of the channels where the turbidity flow spreads out into the lobe formation. This facies covers almost the entire surface of the fan and is associated with the channel-sand facies. The gamma ray log associated with the lobe sand facies shows a funnel shape. The facies is coarsening upward with gamma ray values higher than the channel-sand facies.

In the inner fan, the channel-sand facies is associated with levee forming a channel-levee system. Levee facies deposits through the mechanism of spill by turbidity currents that spreads further from the channel progressively. Levee and lobe have similar character of gamma ray logs and reservoir properties (porosity and permeability). Therefore, to simplify the simulation process, levee deposits are merged into the lobe-sand facies.

The outer part of the lobe-sand facies are sheet-sand facies which spread over a large area of the fan. Sheet-sand facies have a lithology of fine sand interbedding with hemipelagic mudstones. The mudstones including hemipelagic, pelagic, countoritic, and turbiditic mudstones merge into the background shale facies which has high gamma ray values.

Seven submarine fans are identified based on the interpretation described above (Figure 4-1). These stacked fans are separated by shale layers as shown in Figure 4-2.

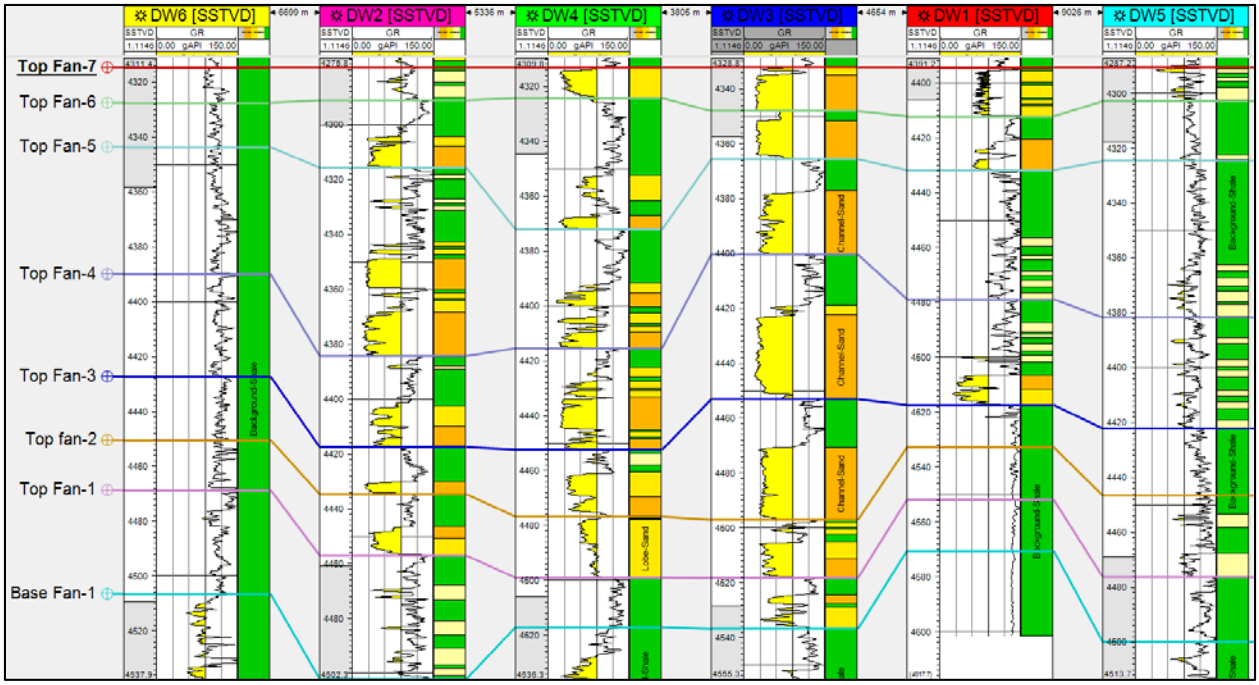

Figure 4-2 Seven submarine fan bodies are identified separated by major shale layers.

4.3 Building of the Conceptual Model

As shown in Figure 4-3, seven depositional models are created based on the relationship between the facies described by the well logs (Figure 4-2).

The sources of material deposited into the deep-water basin may be from deltas, shallow marine shelf areas, or upper slope sediments. The sediments may have a similar composition like the deltaic channels and might be reworked by wave and tide processes. These materials delivered by turbidity currents through the feeder channels deposit further out to the distal and marginal part.

Feeder channels are part of the upper fan consisting of channel-levee system deposits with braided to low-sinuosity channels. This system typically deposits coarse sand and gravel as channel fill creating a channel-levee complex. In this model, the feeder channel comes from northwest direction and deposits to the southeast.

In the mid-fan, depositional lobe units are deposited in form of a simple progradational geometry with turbidity current event that is similar to the upper fan. This progradational trend continues until the channels avulse where accommodation space is available or following the slightly steeper gradient of the lower part of the fan.

The outer portion of the submarine fan system is the lower fan where the terminal sheets are deposited by low magnitude turbidity currents spreading out of the fan. In general, the terminal sheet is a continuation of the depositional lobe, but it is not restricted to the submarine fan deposits.

The basin plain is an area starved of sand. In this area, mudstone or claystone of pelagic and hemipelagic deposits prevail. Sediments are not deposited by turbidity current, but through the suspension.

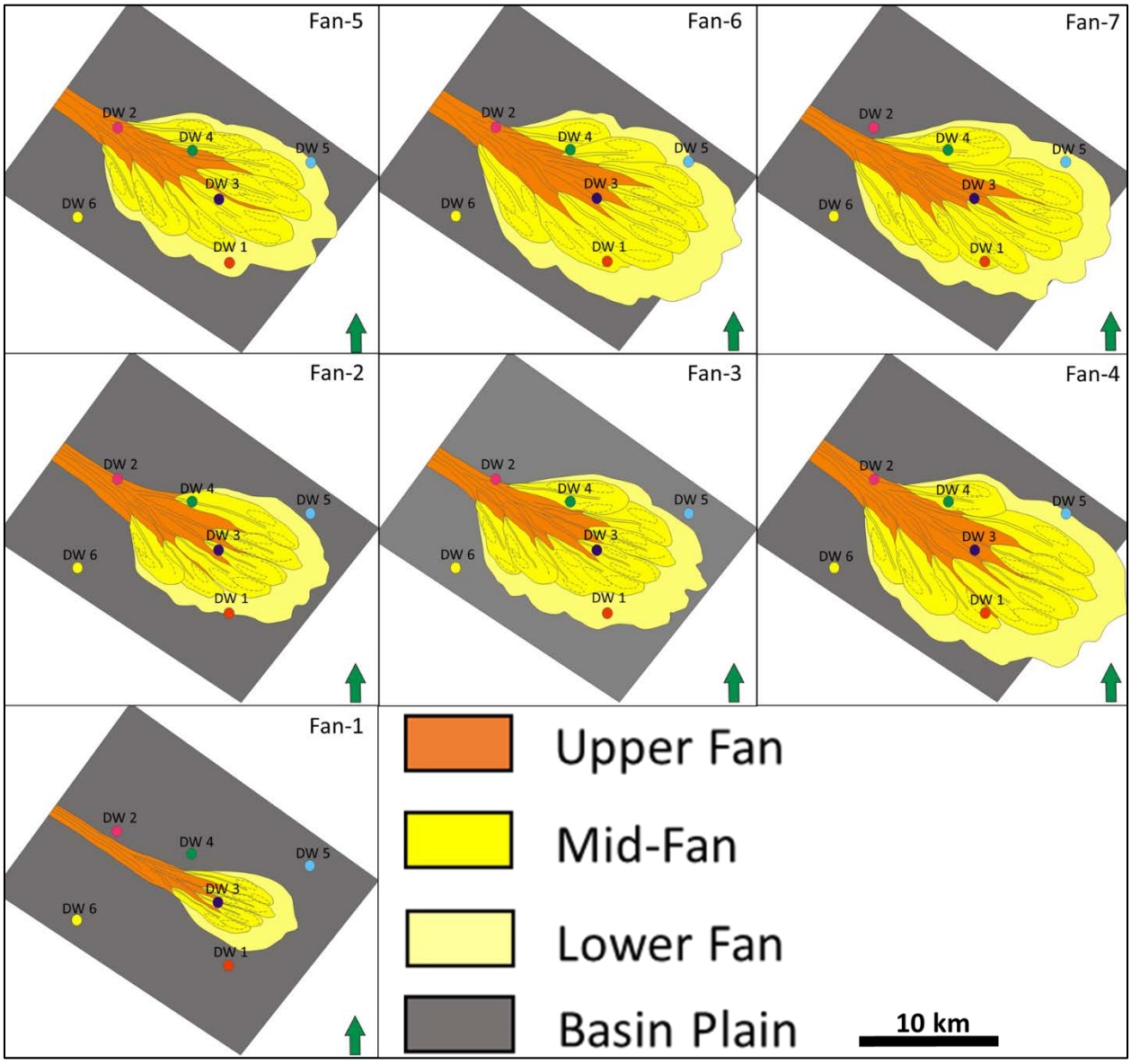

Figure 4-3 The depositional model of seven fan deposits based on the interpretation and lateral facies relationship showing the sub-environment and depositional system.

4.4 Definition of Modelling Region

The deposition model are converted into model regions. This allows doing a facies simulation based on different sets of parameters for each region. The facies deposited in the same sub-environment are genetically related to one another which is called the facies association. The concept of facies association of this study refers to the classification given by Ravnås et al. (2014) which is used to define model regions as shown in Figure 4-4. These models consist of channel belts, channel to lobe transition, central lobe, peripheral lobe, lobe fringe, and background region.

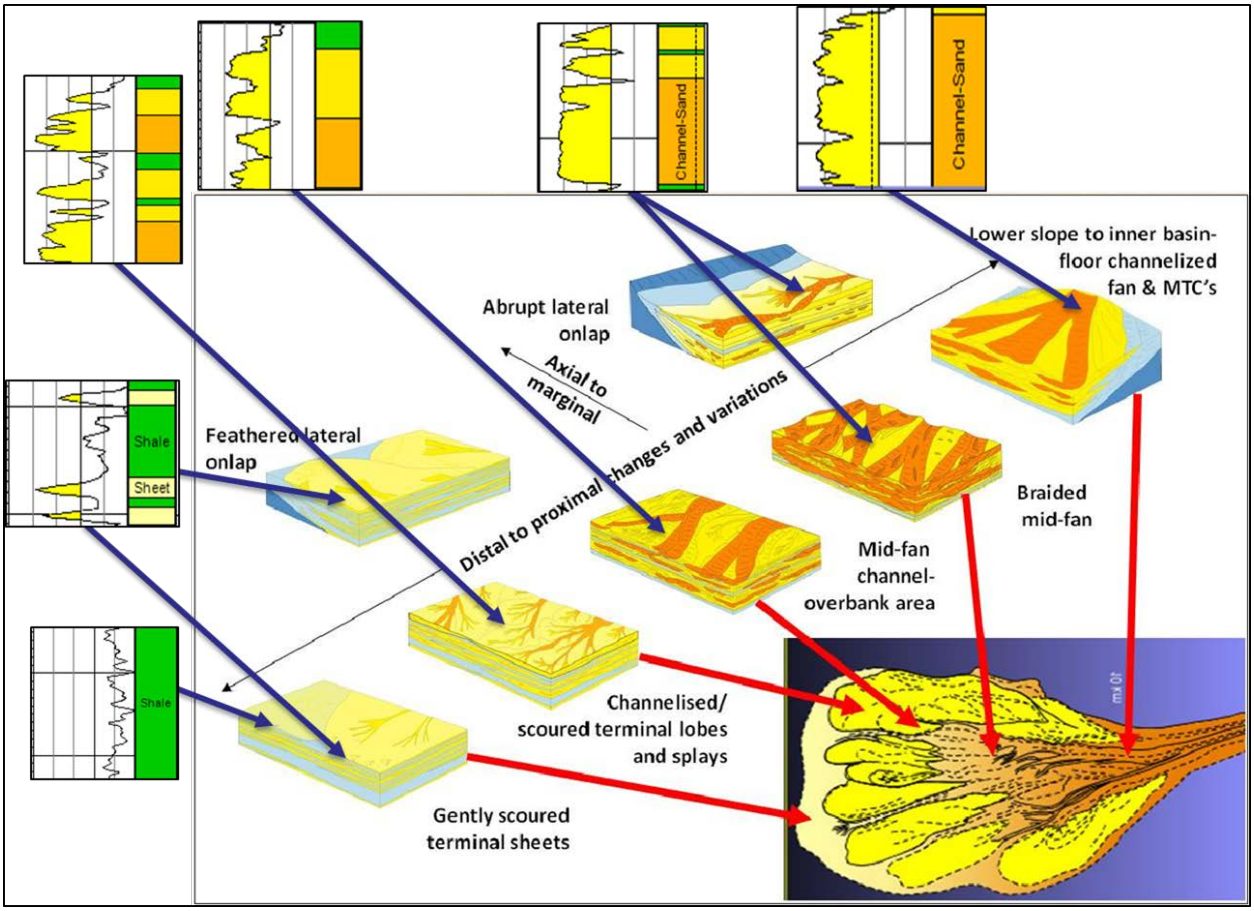

Figure 4-4 The gamma ray logs from the well data correspond to facies association and architecture described by Ravnås et al. (2014).

The channel belt region consists of submarine channel-fill and levee deposits. This region is characterized by erosion at the bottom and stacked amalgamated bed sets of sandstone while the upper part is covered by hemipelagic mudstone.

The amalgamated and scoured bed sets of sandstone are dominating the channel to lobe transition lithology. Channel-sand facies and lobe-sand facies are the main facies building the sandstone

strata in this region that is also called the braided channelized lobe region (Ravnås et al., 2014). Hemipelagic mudstone embedding the bed sets are reflecting variable event of channel filling and avulsion or lateral migration of lobe.

Typically, the central lobe region consists of layered to amalgamated sandstones which are relatively coarse-grained. This region represents alternating channelized or scouring deposits caused by the depletion of the turbiditic flows. The geometry of this region resembles mounds suggesting vertical variation in bedding. Hemipelagic sediments are also coverering the top of this region.

In the peripheral lobe region, the lithology consists of layered packages of sandstones separated by thin mudstones. This region covers the central to the lower part of the mid-fan area.

The lithology of the fringe lobe region consists of thin-bedded to medium-bedded sandstones embedded in hemipelagic mudstone. This region represents the marginal and distal parts of the lower fan area. The sheet-sand facies have nearly equal amounts of background-shale facies.

The background region is mainly covered by background-shale facies of deep marine mudstones or claystones, based on allogenic mechanism. Laterally, this region is equivalent to the basin plain of the depositional model, while in vertical succession; this region is composed of hemipelagic mudstone. Figure 4-5 shows the modelling region for the seven submarine fans.

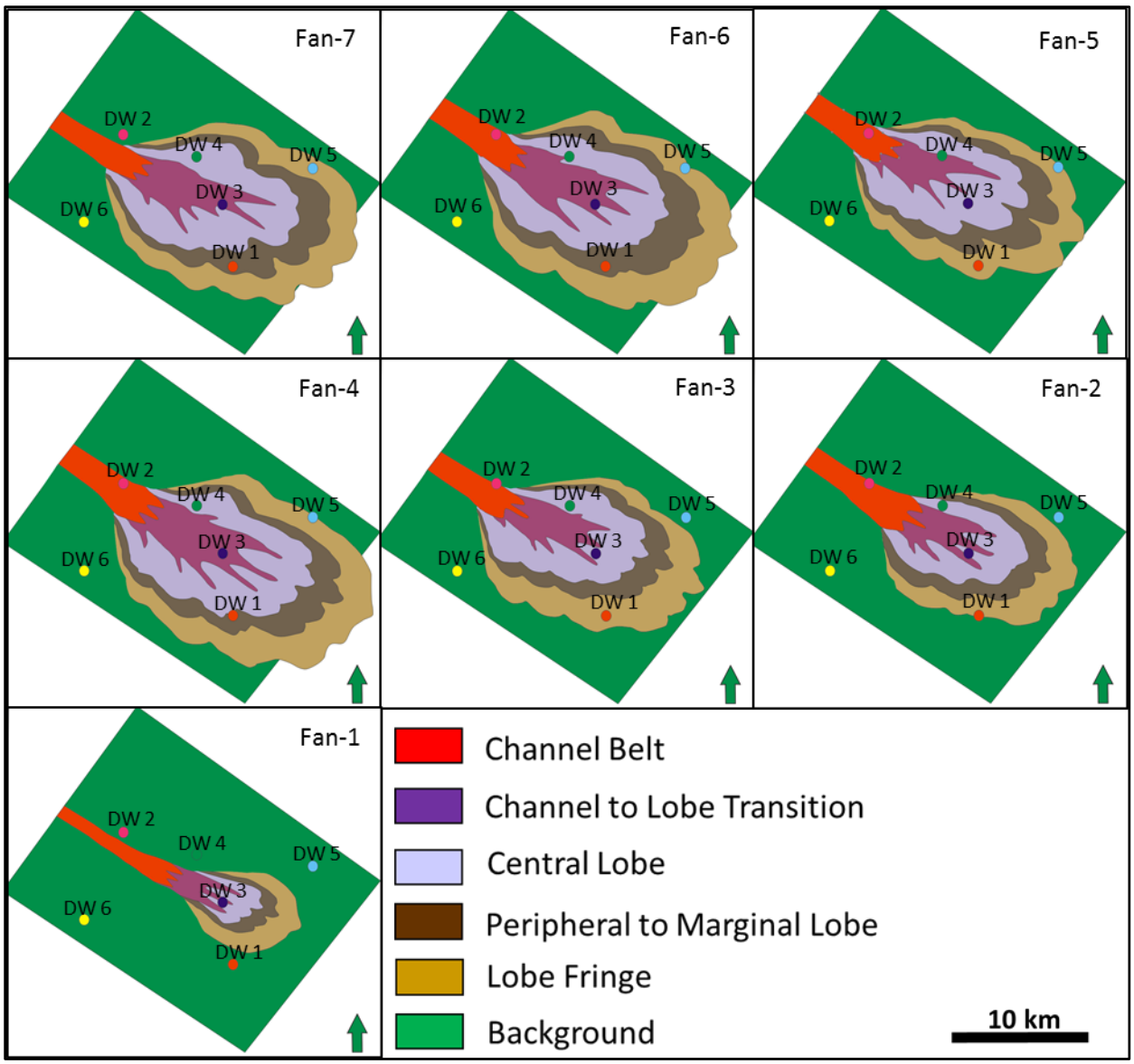

Figure 4-5 Modelling regions of seven submarine fans.

4.5 Training Images Concept for the Study Area

MPFS utilizes training images as the main input in order to conduct the facies simulations. Training images can be defined at any scale provided they take the model resolution into account, which in this study is 150x150x2 m in X/Y/Z directions. For example, if the channel width is 4 grid cells wide in the training image, the simulated channel width of the facies model will be 4x150=600 m. This applies to each X/Y/Z direction. Consequently, one grid cell in the training image equals to one grid cell in the simulation grid.

For the channel-sand facies, the thickness of the channel can be determined from the facies logs. The width of the channels is obtained by the empirically derived relationship between the channel thickness and channel width given by Fielding & Crane (1987) (Figure 4-6). The channels of submarine fan deposits are braided and show a low sinuosity corresponding to the criteria of case1B of Figure 4-6. Based on this analogue data, the width of the channel of the model ranges from 9 to 638 m for a channel thickness range between 6 and 25m.

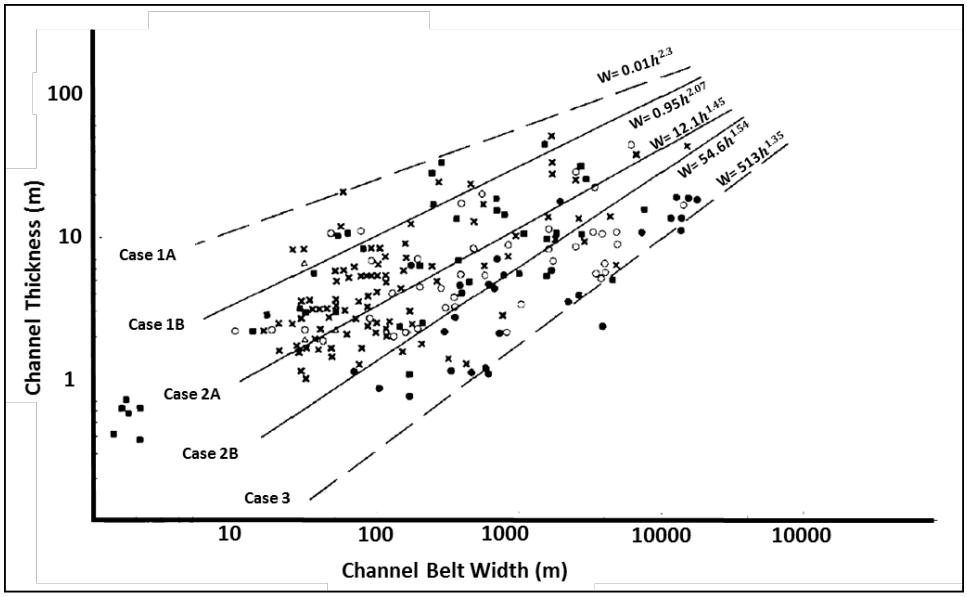

Figure 4-6 The plot of the relationship of the channel thickness and channel width (Fielding & Crane, 1987)

Each model region has a different channel width and channel pattern (Figure 4-7a – 4-7c). The channel belt region has channels of a width of up to 600 m or four grid cells of the simulation grid. The channel pattern of this region is sub-parallel and individual channels may intersect each other. This is because during the process of formation the channels are free to migrate since the levee walls cannot hold the turbidity current of the channel. Thus, the levee deposits occur in the area between the channels. The channel to lobe transition region has a channel width of ca 300 m equivalent to two grid cells of a simulation grid. The character of the channels in this region are similar to the channel belt region. However, the density of the channels is sparse. The channels in this region start to show avulsion to form a depositional lobe. This is especially noticeable in the central lobe region where the channel spread follow the surface of the deep marine. The peripheral to marginal lobe region and lobe fringe region have a channel width below the lateral grid

resolution or less than 150 m, and consequently the training image of this region does not contain channels. For the background region, no channels are created during deposition.

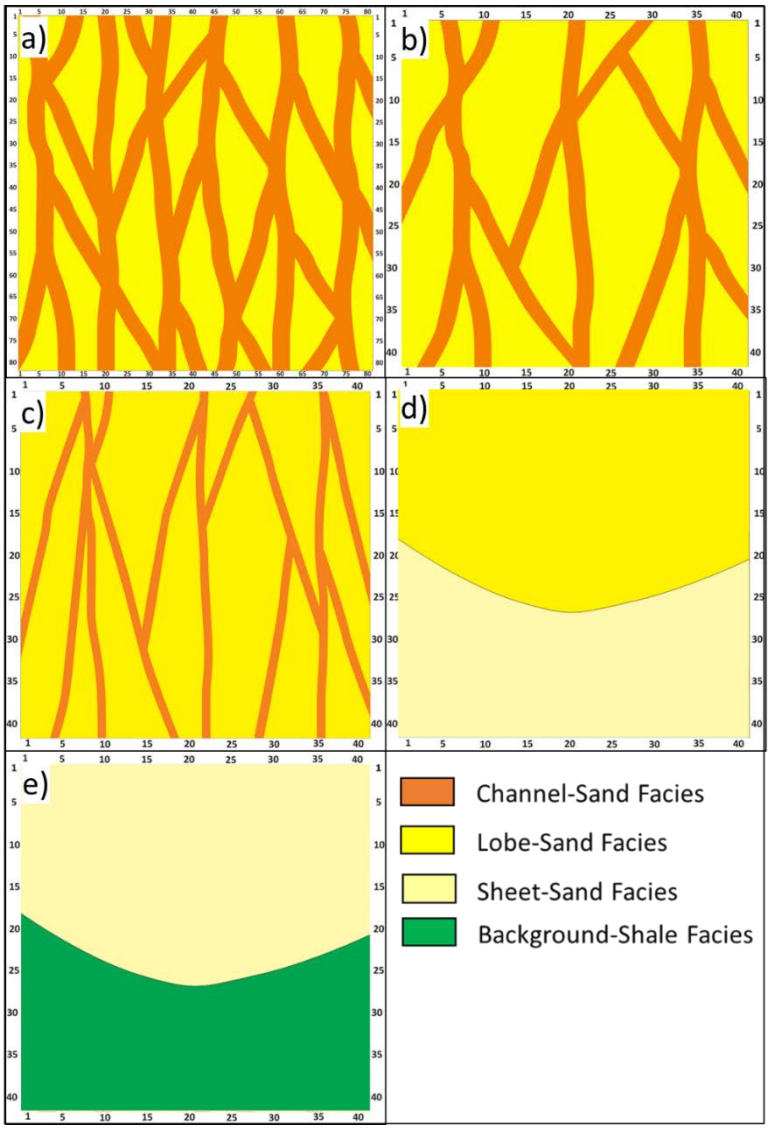

Figure 4-7 Training images concepts for each region a) channel belt region b) channel to lobe transition region c) central lobe region d) peripheral to marginal lobe region e) lobe fringe region.

4.6 Building of Facies Model

4.6.1 Editing Simulation Grid

This study has seven zones which consist of seven individual fans resulting from the well top interpretation. The well tops defining the zone tops and bases are converted into surface maps using an interpolation algorithm. These surfaces are used as input for creating the zones of the 3D

grid. Finally, each modelled zone is sub-divided into layers that have an average thickness of two meters (Figure 4-8).

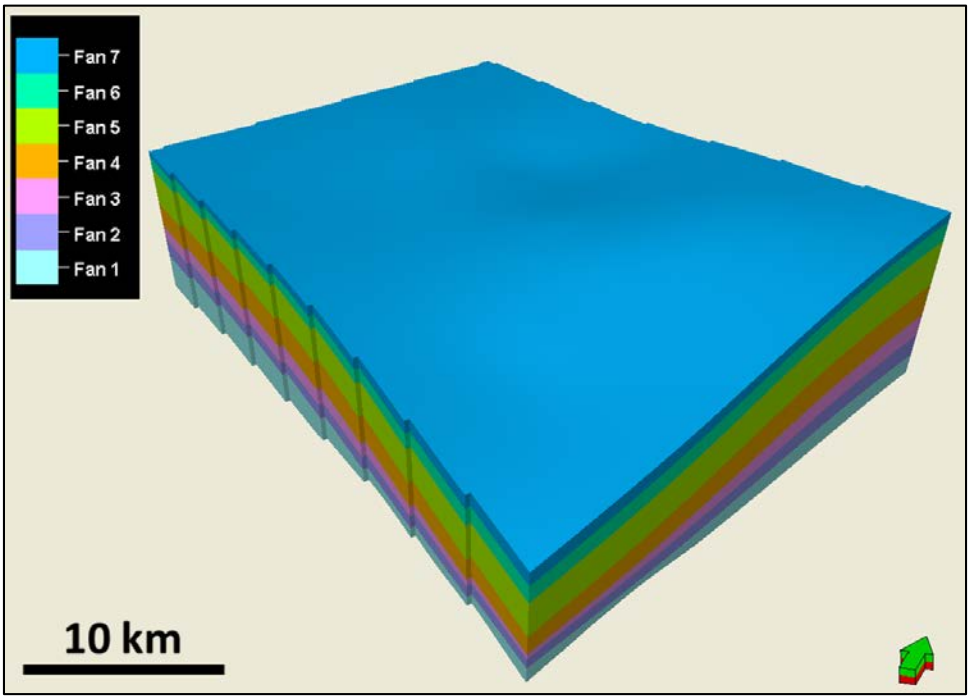

Figure 4-8 The simulation grid showing seven zones of submarine fans.

4.6.2 Creating Training Image

The setup of the training images is based on the training image concept previously described. Ideally, the training image must be set up in 3D to reflect the vertical and lateral distribution of the facies. A single layer training image can also be used for facies modelling, however they do not allow to control the vertical facies distribution. The advantage of single layer training images is that the MPFS is much quicker compared to utilizing multilayer training images. In order to create single layer and multilayer training images, several techniques can be utilized, for example, unconditioned object modelling or facies drawing using paint-brushing tools. Furthermore the orientation of the training image must be along the north-south direction (azimuth = 0^o) to perform the local rotation of facies patterns (Zhang, 2009). Four groups of training images are created which are input to the four MPFS methods discussed in this thesis.

a. Single Layer Training Images of Two Facies

First, two different sizes of training image grids are created. The training image of the big grid, which has 81x81x1 cells, allows to capture the channel pattern of the channel belt region. This

region has the largest channel width of 600 m (4 pixels) of all discussed regions. The small grid, which has 41x41x1 cells, is used to create five training images for all other regions. This grid size is suitable enough to capture the pattern of the facies. Figure 4-9 shows the process of making single layer training images of two facies using the facies drawing technique.

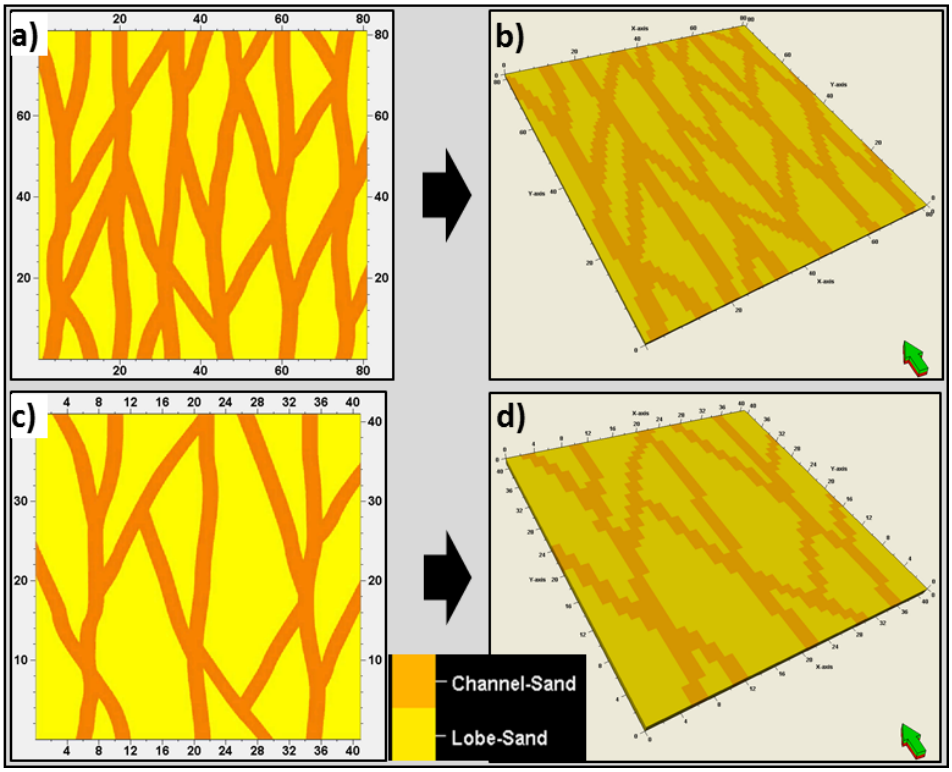

Figure 4-9 The process of creating training images by using paint-brushing tool to draw the facies on the training image grid. a) The training image concept for channel belt region b) The grid result of the 81x81x1 cells c) The training image concept for central lobe region d) The grid result of the 41x41x1 cells.

b. Multilayer Training Images of Two Facies

The concept of multilayer training images of two facies is based on the relationship between the channel thickness and channel width given by Fielding and Crane (1987). Based on the previously discussed training image concepts, the channel pattern of this group is similar to the group of single layer training images of two facies. The difference between these two groups is the thickness of the facies as shown in Figure 4-10.

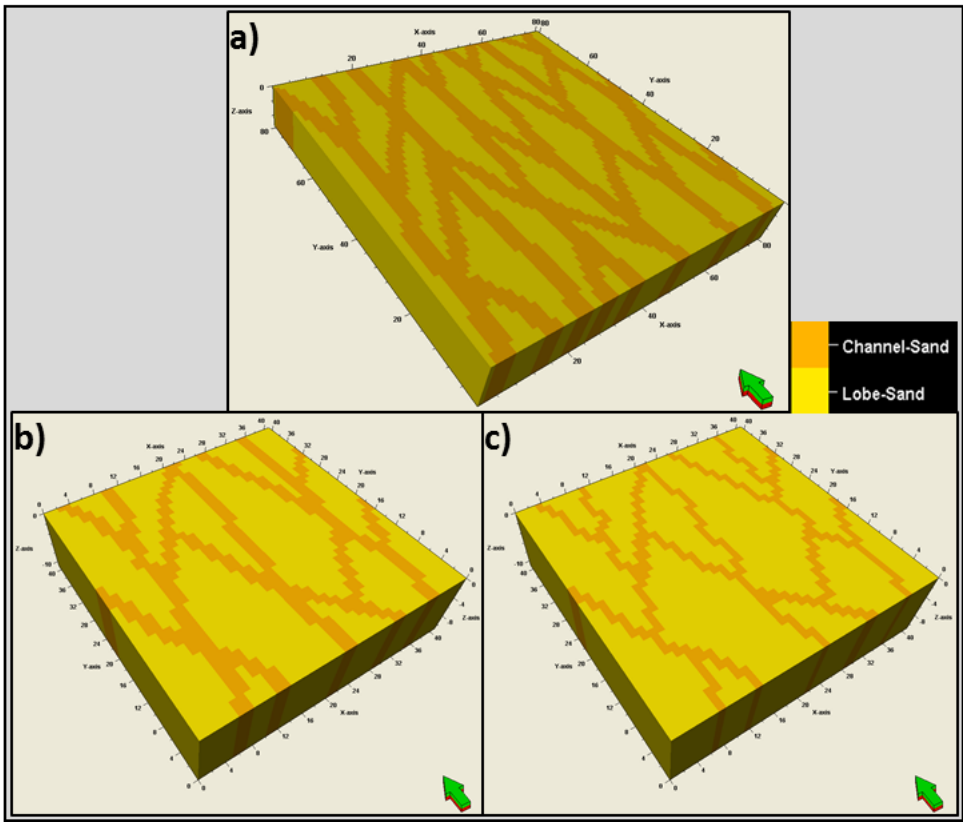

Figure 4-10 Examples of multilayer training images of two facies a) Training image with 81x81x11 grid cells which models channels of four pixels (600 m) width and eleven pixels (22 m) thickness for the channel belt region b) The 41x41x8 grid with channels of two pixels (300 m) width and eight pixels (16 m) thickness for the channel to lobe transition region c) The 41x41x6 grid cells for channels of one pixel (150 m) width and six pixels (12 m) thickness of channel-sand facies for the central lobe region.

c. Multilayer Training Images of Three Facies

This group of training images represents the vertical succession of submarine fan deposits. Every training image is covered by background-shale facies as shown in Figure 4-10. The size of the training image grid of this group follows the grid size of the group of multilayer training images of two facies.

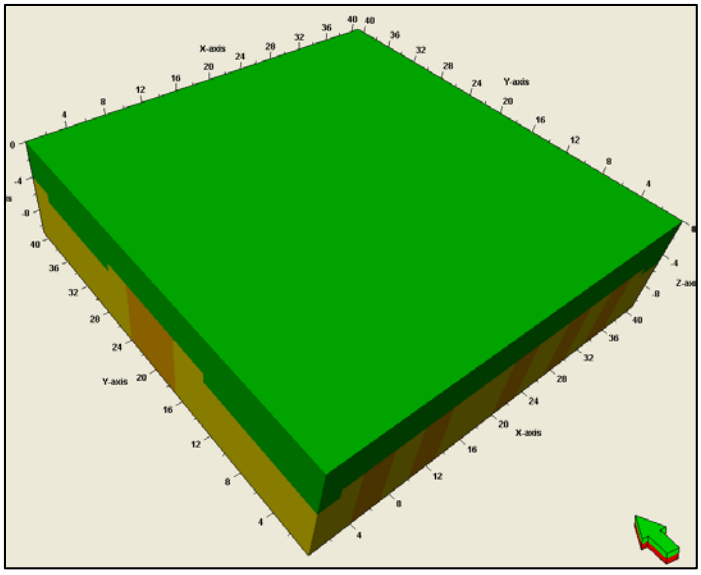

Figure 4-11 An example of 3D training image of three facies for channel belt region.

d. Multilayer Object Modelling Training Images

The unconditional object-based modelling allows to generate training images in multilayer using the geometry information of the object modelling. The size of the facies can be controlled by the geometrical parameters, for example channel width, sinuosity level, fan width, and the direction of the deposition. This group of training images is created using 41x41x11 grid cells. Figure 4-12 is showing examples of training images using unconditioned object modelling

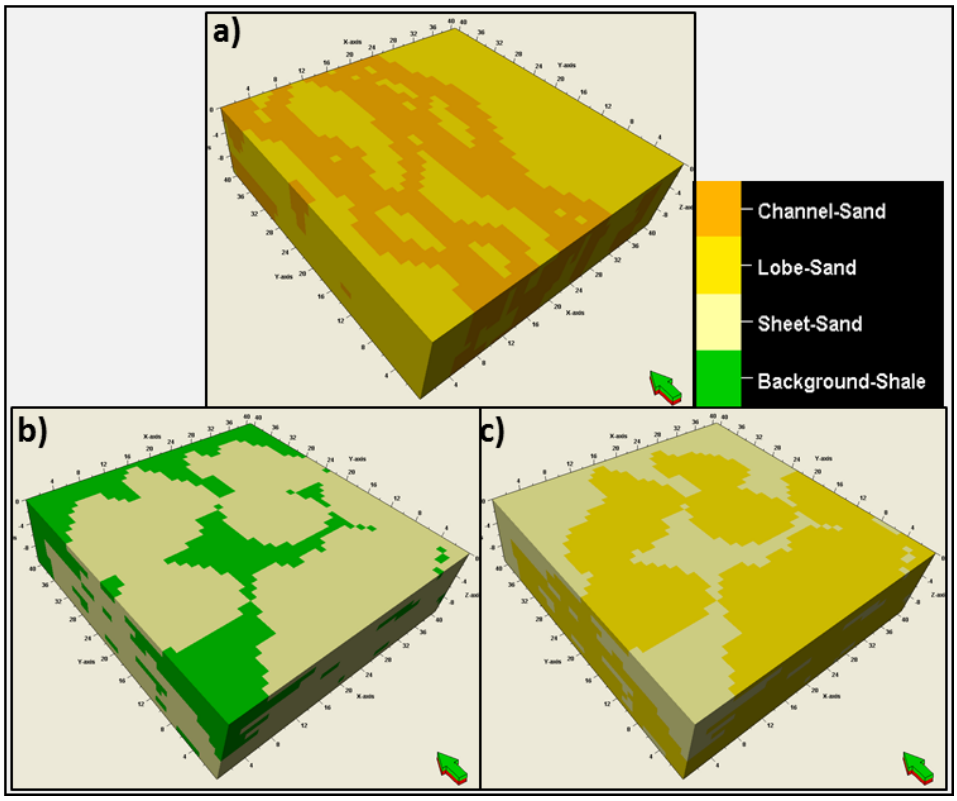

Figure 4-12 Examples of 3D object modelling training images a) The training image for channel belt region b) The training image for lobe fringe region c) The training image for peripheral to marginal lobe region.

4.6.3 Physical Region

Figure 4-13 illustrates the procedure of creating the physical region of a 3D grid. This process begins by importing images of the modelling region concepts that are created in drawing software. The images are converted to maps by using a surface resampling algorithm. In this way seven physical regions for each fan are converted to maps and subsequently modelled into the 3D grid. However, the facies boundary of the physical region at this stage does not show the progradational trend previously described. Therefore, the truncated Gaussian simulation (TGS) with a trend is applied which allows to create the geometry of progradational facies. The last stage of this process is to edit manually the result of TGS. The editing process is done based on the facies relationship in the study area where the edited physical region does not clash with the facies of well data.

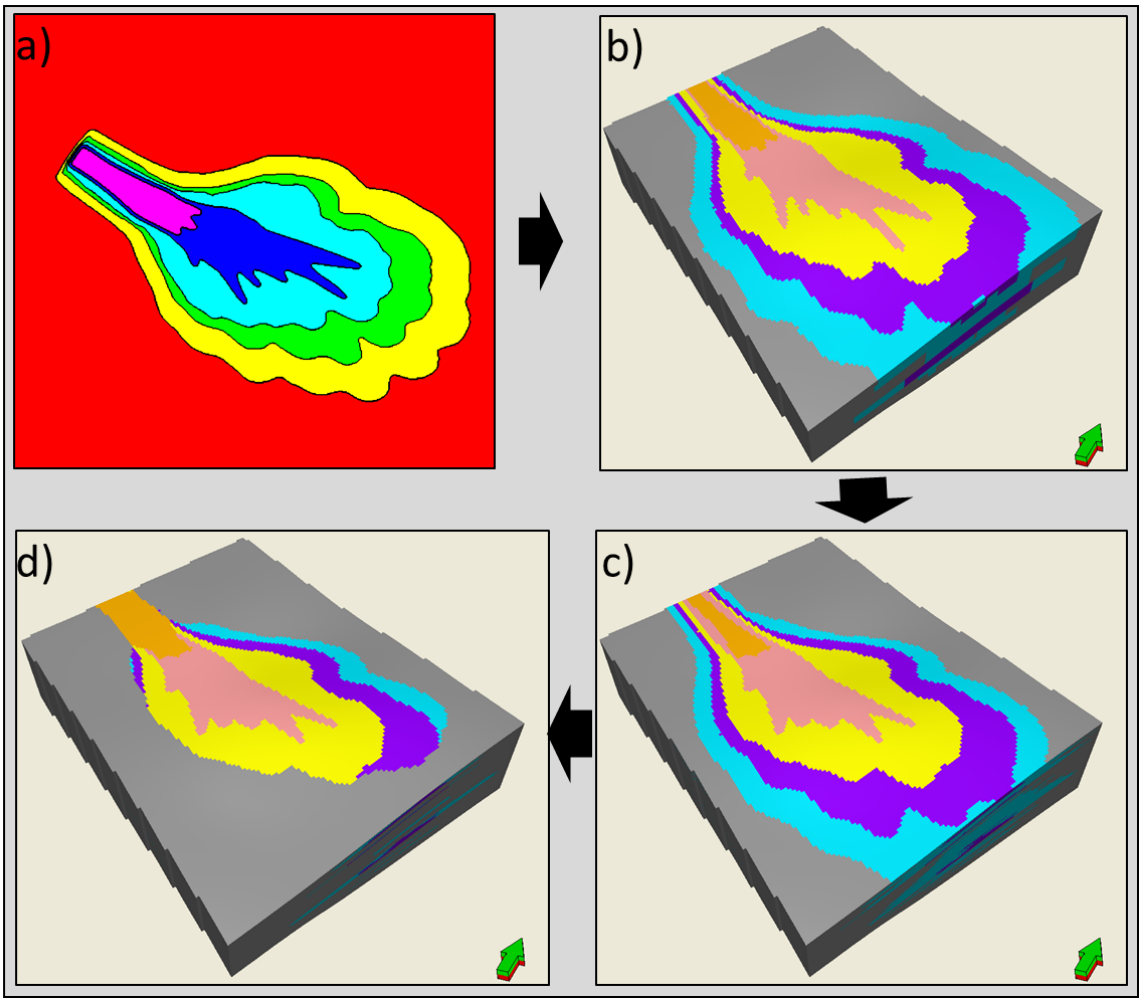

Figure 4-13 The process of the physical region creation a) Map of the physical region b) 3D grid of physical region after combining all the maps showing a blocky boundary between region c) 3D grid of physical region using truncated Gaussian simulation (TGS) to to produce the progradational pattern d) Deterministically edited physical region which is controlled by vertical and lateral facies relationship.

4.6.4 Azimuth/Orientation of Facies Distribution

The procedure to create the azimuth/orientation input is illustrated in Figure 4-14. The initial stage of making this additional input is by drawing a polygon in accordance with the directions of the deposition for the physical region map. The polygon directions describe the azimuth property corresponding to the direction of the channels. These polygons are then converted into maps by interpolating the azimuth values assigned to each polygon. This process is applied for all channels of the seven submarine fans. The last stage is combining these azimuth maps into a 3D grid property.

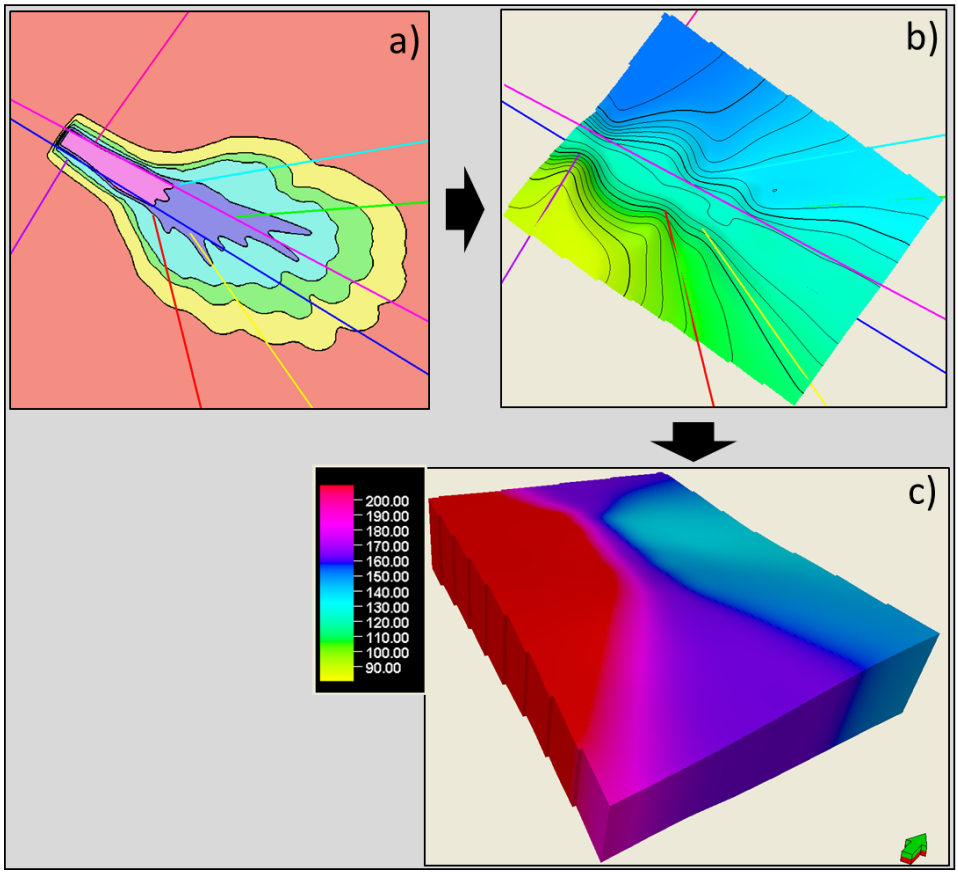

Figure 4-14 The process of making an azimuth/orientation grid property a) Polygons of the orientation b) Map generated from polygons c) 3D grid of the azimuth properties.

4.6.5 Facies Probability

The facies probability is used as the soft data in MPFS. In this study, there are two types of facies probability: the trend modelling and the vertical proportion. The trend modelling is based on the facies distribution given by the well data and controlled by the boundary of the physical region (Figure 4-15).

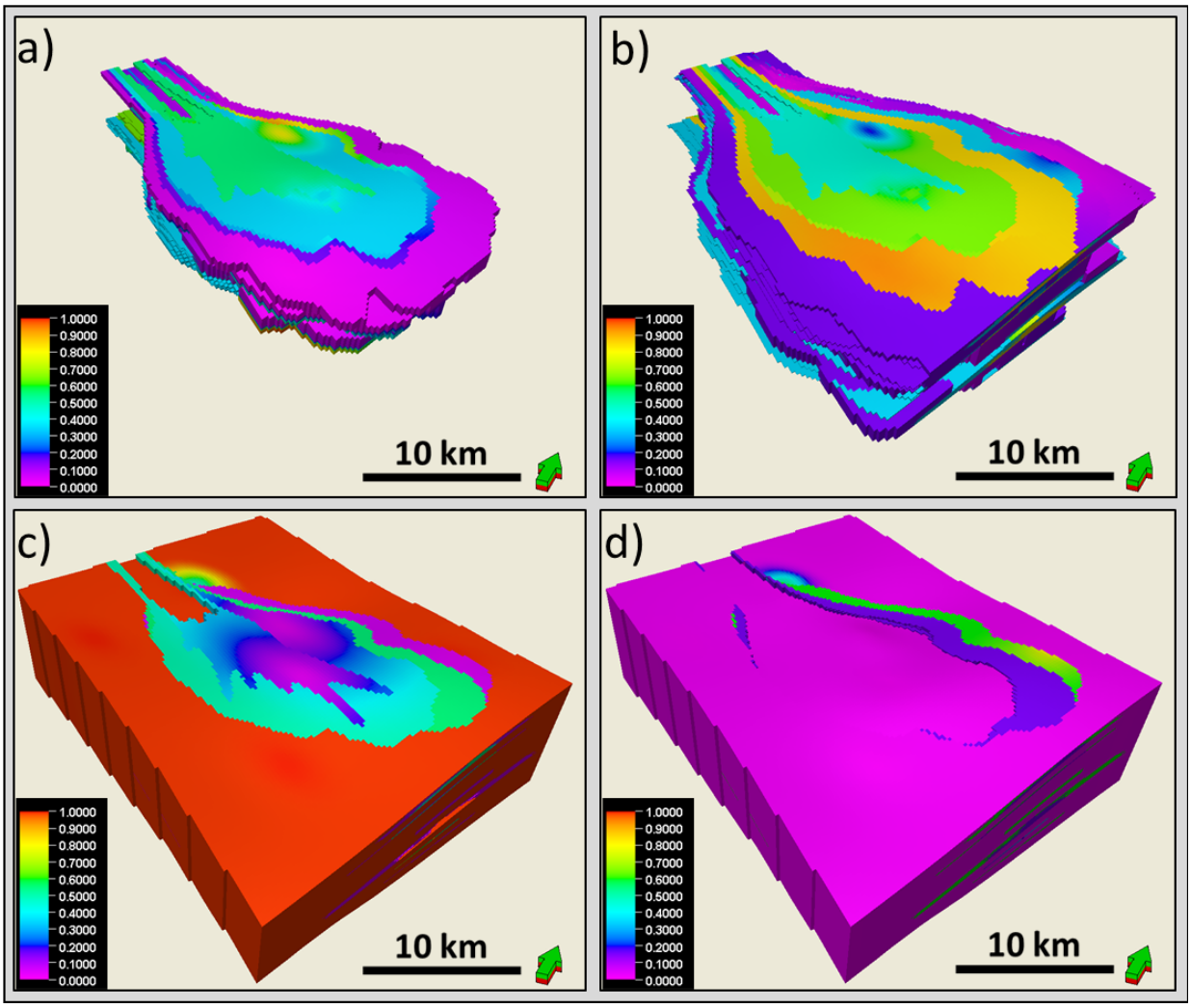

Figure 4-15 Probability cubes derived from trend modelling a) The probability cube of channel-sand facies b) The probability cube of lobe-sand facies c) The probability cube of sheet-sand facies d) The probability cube of background-shale facies.

The vertical proportion is derived from the facies logs for each zone. Figure 4-16 shows an example of the vertical proportion for the facies probability.

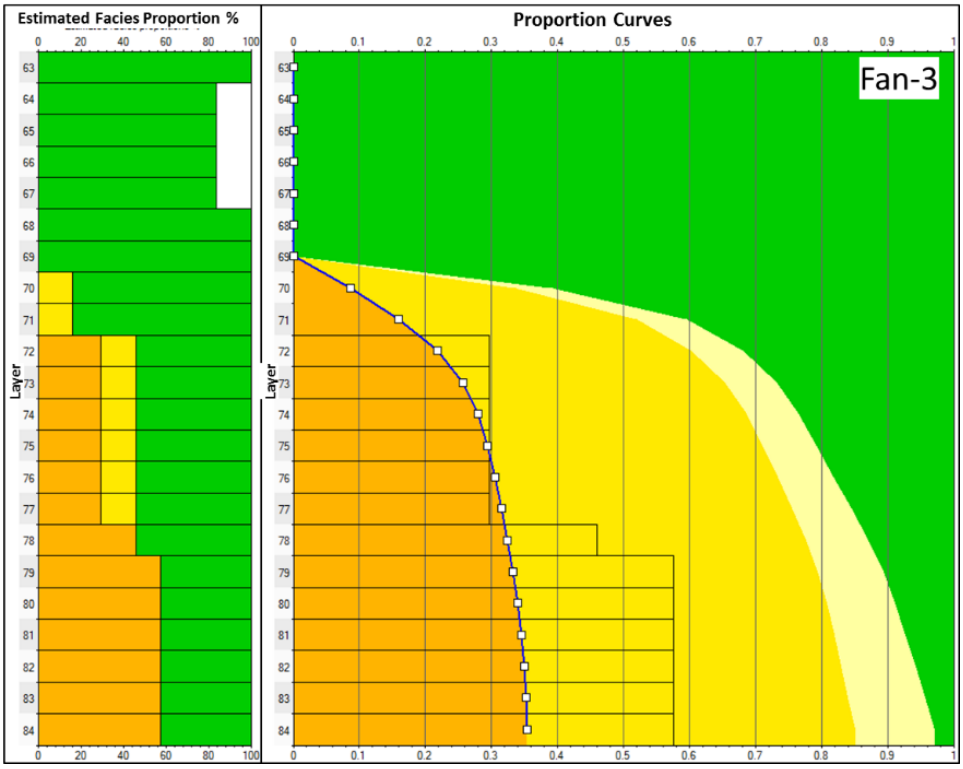

Figure 4-16 An example of facies probability using vertical proportion.

4.6.6 Multi-Point Facies Simulation (MPFS)

The MPFS is the final step of a multi-point statistics (MPS) facies modelling. Four MPFS models are carried out by using the described four groups of training images (Figure 4-17 – 4-20). In order to compare the four methods, the facies fraction of the modelled channel-sand facies must be similar for all four methods. For the channel belt region, the target facies fraction of channel-sand is 45%. The channel-to-lobe transition region has a target channel-sand facies fraction of 25%. Lastly, the central lobe region has a fraction of 15% for channel-sand.

Three methods are simulated using the same additional input which are edited physical region, azimuth/orientation cube, and facies probabilities from trend modelling. The three methods are method I using single layer training images of two facies, method II using multilayer training images of two facies, and method IV using multilayer training images based on object modelling. The method III uses multilayer training images of three facies as the main input. Moreover, the additional inputs that are used for method III are the physical region derived by TGS, azimuth/orientation cube, and the facies probabilities from vertical proportion curves.

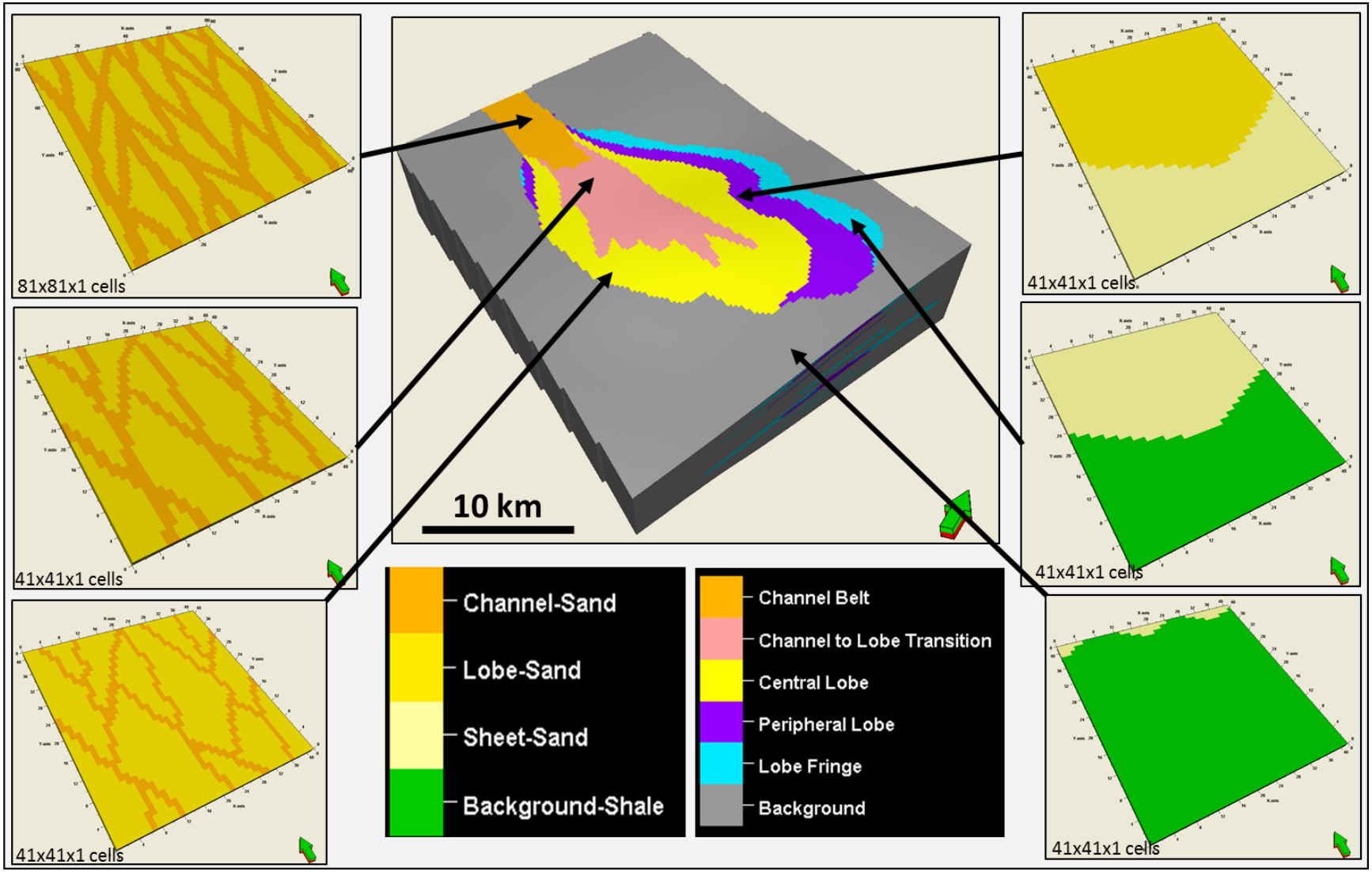

Figure 4-17 MPFS method I using a group of single layer training images of two facies and the edited physical region.

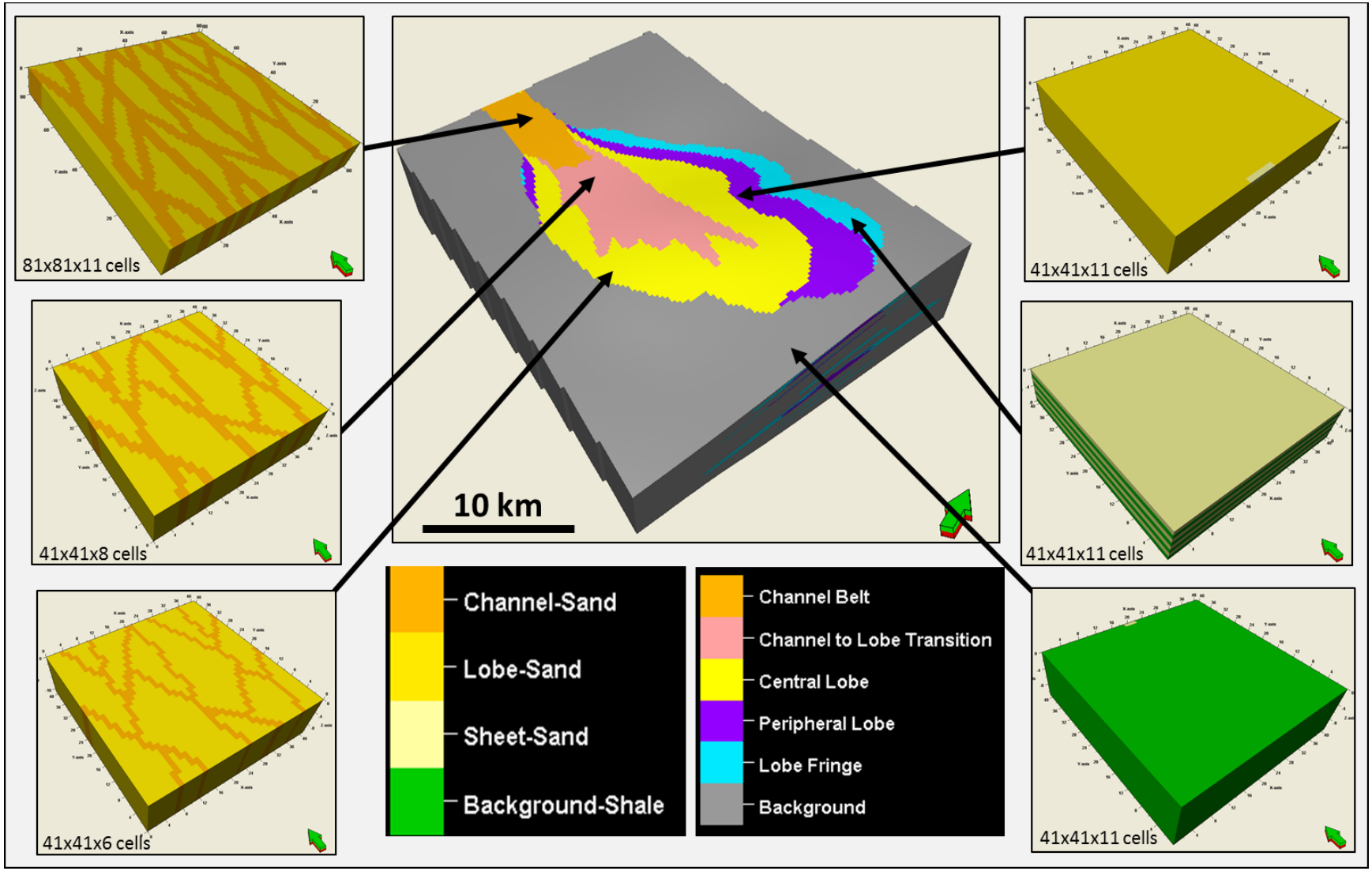

Figure 4-18 MPFS method II using a group of multilayer training images of two facies and the edited physical region.

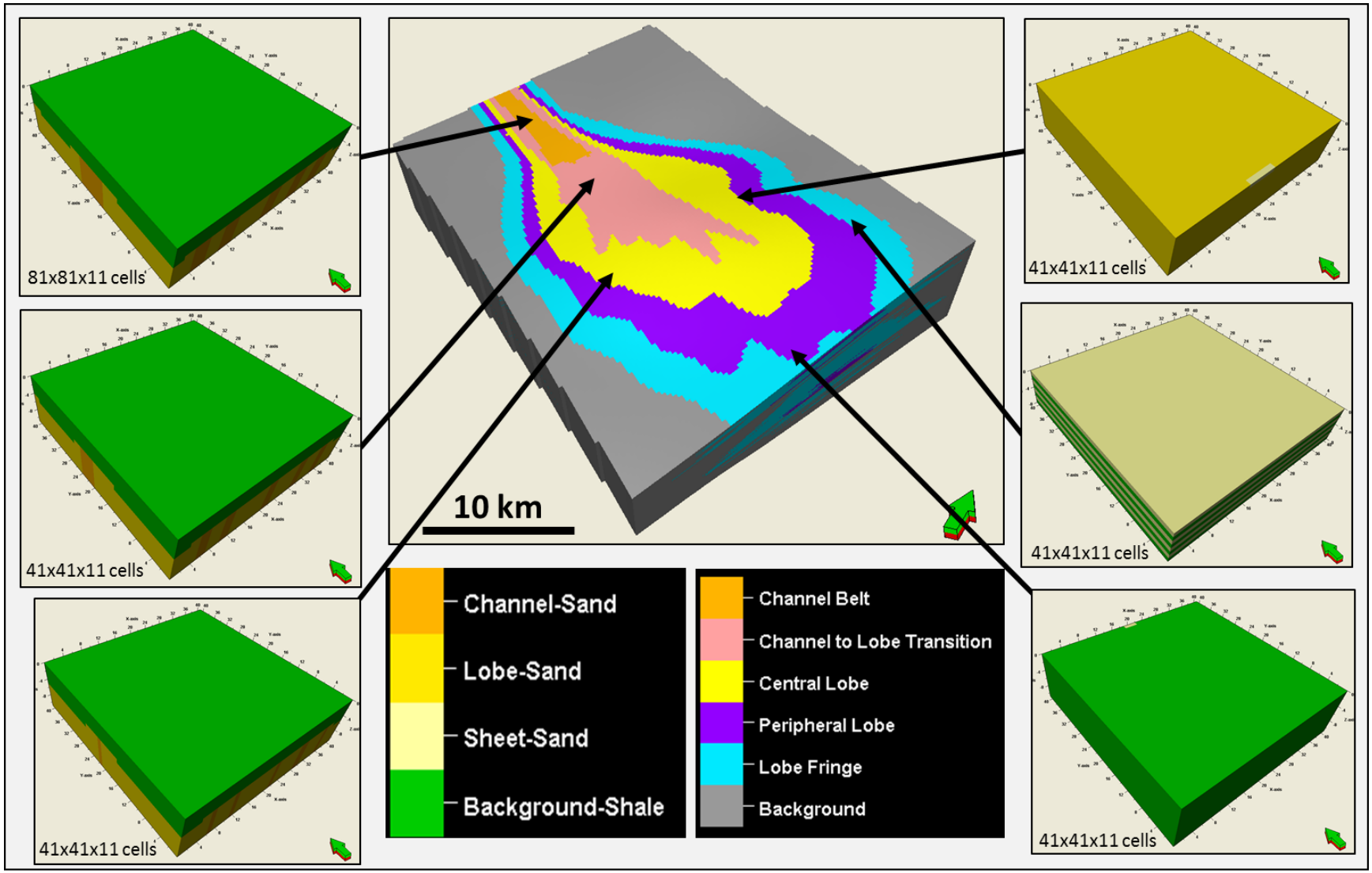

Figure 4-19 MPFS method III using a group of multilayer training images of three facies and the physical region of TGS result.

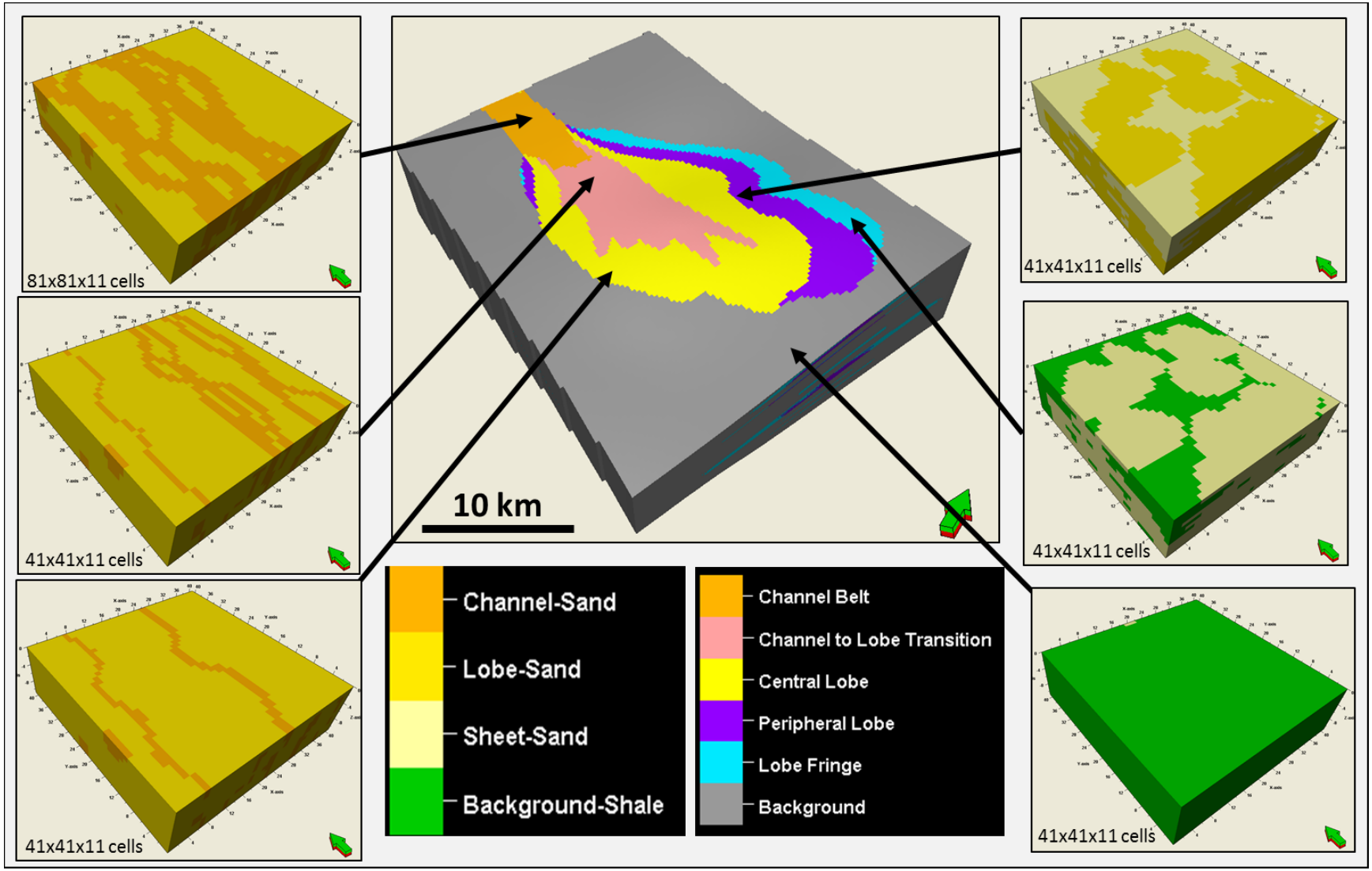

Figure 4-20 MPFS method IV using a group of multilayer training images based on object modelling and the edited physical region.

4.6.7 Gauss Indicator Simulation Facies Modelling

The pixel-based facies modelling is using Gauss indicator simulation (GIS). This technique employs a variogram model as main input and the conditioning data as secondary input. The variogram analysis does not allow deriving a reliable variogram model because of lack of well data. The horizontal ranges were selected such to mimic stretched sand bodies oriented in the general channel direction. The vertical variogram range was set between 12 and 22 m reflecting the typical channel thickness derived from the log data. In order to compare the GIS method with the MPFS method, the used input facies fractions of MPFS are assigned to GIS. Also, the edited physical regions of MPFS are used in GIS. Each physical region gets its own input facies distribution and variogram model. Table 4-1 shows the parameters assigned to each region in GIS.

Table 4-1 GIS parameters

Region		Channel belt	Channel-to-lobe transition	Central lobe	Peripheral lobe	Lobe fringe
Facies fraction (%)	Channel-sand	45	25	15		
	Lobe-sand	65	75	85	85	
	Sheet-sand				15	75
	Background-shale					25
Variogram	Type	Spherical	Spherical	Spherical	Spherical	Spherical
	Major direction (m	3000	3000	3000	3000	3000
	Minor direction (m	1500	1500	1500	1500	1500
	Vertical (m)	22	16	12	8	6
	Azimuth (degree)	-70	-70	-70	-70	-70

4.6.8 Object Modelling

The object modelling is used to create the channel-sand facies with lobe-sand facies as background. For peripheral lobe and lobe fringe regions, the fan lobe object is used to simulate lobe-sand facies and sheet-sand facies. The geometry and the facies fraction of this facies modelling follow the corresponding object based training images of the MPFS method and are shown in table 4-2, table 4-3 and table 4-4. For the orientation of the channel-sand facies, object modelling is using the input orientation used by the MPFS method. Similar to the GIS method, the object-modelling method also uses the edited physical region as conditioning data.

Table 4-2 Types of object and facies fraction that are used for object modelling.

Region	Type of Geometric Body			Background	
	Type	Facies	Fraction (%)	Facies	Fraction (%)
Channel belt	Adaptive channel	Channel-sand	45	Lobe-sand	55
Channel-to-lobe transition	Adaptive channel	Channel-sand	25	Lobe-sand	75
Central lobe	Adaptive channel	Channel-sand	15	Lobe-sand	85
Peripheral lobe	Fan lobe	Lobe-sand	85	Sheet-sand	15
Lobe fringe	Fan lobe	Sheet-sand	75	Background-shale	25

Table 4-3 Parameters of adaptive channel object modelling.

Region	Channel belt region	Channel-to-lobe transition region	Central lobe region
Amplitude (m)	600-1000	600-1000	400-800
Wavelength (m)	1000-2000	1000-2000	800-1200
Relative sinuosity (fraction)	0.1	0.1	0.1
Channel width (m)	600	300	150
Channel thickness (m)	10	8	6

Table 4-4 Parameters of lobe fan object modelling

Region	Peripheral lobe region	Lobe fringe region
Minor width	1500-2750	1500-2750
Major/minor ratio	0.8-1.2	0.8-1.2
Thickness	10-20	10-20
Tapering	0.1-0.3	0.1-0.3

3.8 Connectivity Analysis

The connectivity analysis is conducted to analyze the connectivity of facies bodies. This analysis displays the connected cells of the model for a specific facies. In this study, the connectivity of channel-sand facies bodies are calculated to compare the modelling results of the four methods of MPFS, the GIS method, and the object modelling method.

5. FACIES MODELLING RESULTS

Based on the conceptual model, six facies models are carried out using different methods. Four methods use multi-point facies simulation (MPFS). Two additional methods are carried out using Gauss indicator simulation (GIS) and object modelling. This chapter describes the observation of the six facies models resulting from the different methods.

5.1 Multi-Point Facies Simulation (MPFS)

5.1.1 MPFS Method I

The method I of MPFS is using a group of single layer training images of two facies. As additional input, this method uses an edited physical region cube, an azimuth cube, and a facies probability cube based on the trend modelling.

As seen in Figure 5-1a, the three regions that contain channel-sand facies show channels of different width. In the proximal part, the channel belt region is successfully reproduced showing the feeding system of submarine fan. The channel of this region has a large width and low sinuosity. The width of the channel becomes narrower in the channel to lobe transition region starting the branch of feeder channels. Finally, the central lobe region has the narrowest channel spreading over the whole region as seen in the central part of the model.

The other three regions (peripheral lobe, lobe fringe and background region) do not have channel-sand facies and consequently show no complex patterns. The training images for these regions that comprise lobe-sand, sheet-sand and background-shale facies are simple and consequently MPFS does not have any problem in modelling these regions. The sheet-sand facies, which is a continuation of the lobe-sand facies, is well modelled. The background-shale facies that is separating the fans is well reproduced as shown in Figure 5-1b.

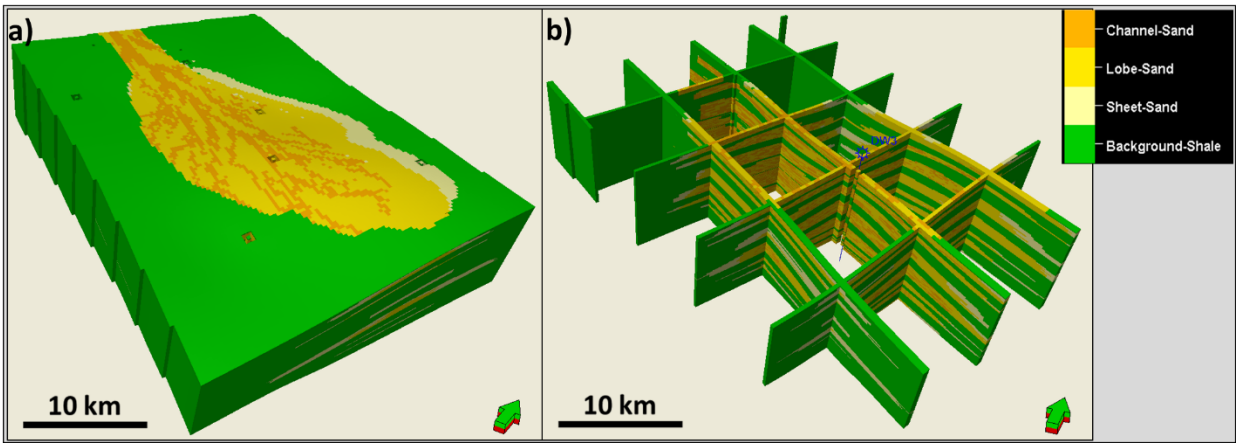

Figure 5-1 The modelling results of the method I using 2D training images with two facies a) Facies model showing the top of fan-7 b) Cross sections thru the facies model showing its internal architecture.

The connectivity analysis shows the degree of connectivity of the channel system for every fan as seen in Figure 5-2a. Each body is distinguished by its unique color. The colors indicate one massive continued and connected channel system for each fan. Figure 5-2b and 5-2c show two cross sections thru the connected channel bodies. The stacked channel of this facies model is not showing the amalgamated channel in the submarine fan system. Therefore, the transition of channel thickness is not well represented in this facies model.

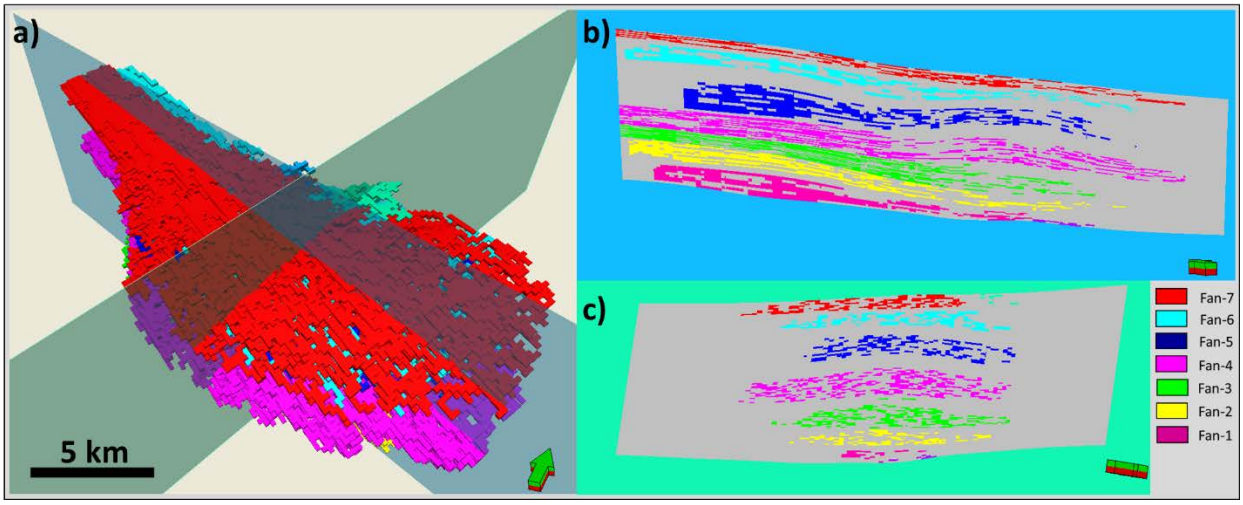

Figure 5-2 The result of connectivity analysis of facies model of first methodology a) The connectivity bodies of channel-sand facies and the position of cross-sections b) Cross-section from proximal part to distal part b) Cross-section from central part to marginal part.

5.1.2 MPFS Method II

The method II of MPFS is using a group of multilayer training images with two facies. An edited physical region cube, an azimuth cube and a facies probability based on trend modelling are utilized as additional input.

Similar to the method I, the channel size is changing from the proximal part to the distal part as shown in Figure 5-3a. The channel is denser compared to the facies model of MPFS method I. The modelling result of the other three regions that do not have any channels are identical to the facies model of method I as seen in Figure 5-3b.

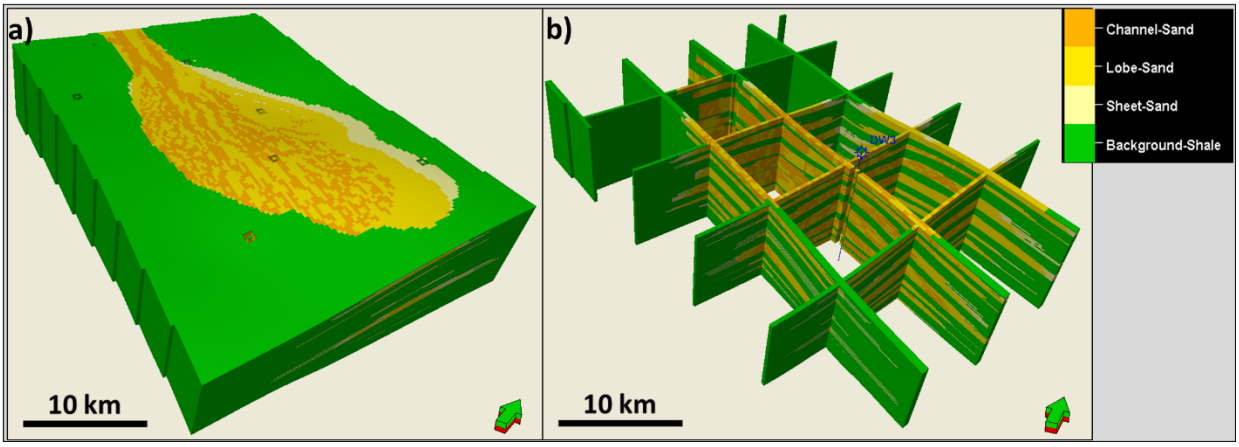

Figure 5-3 The modelling results of method II using multilayer training images with two facies a) The facies model showing top of fan-7 b) Cross sections thru the facies model showing its internal architecture.

The connectivity of the channel bodies is more intense compared to the facies model of MPFS method I (Figure 5-4a). The amalgamated channel is well reproduced in this model. Figure 5-4b shows the transition of the channel thickness from proximal part to distal part where the channel thickness is getting thinner compared to the proximal part. Figure 5-4c displays the transition from the central part to the marginal part where the channel thickness is becoming thinner.

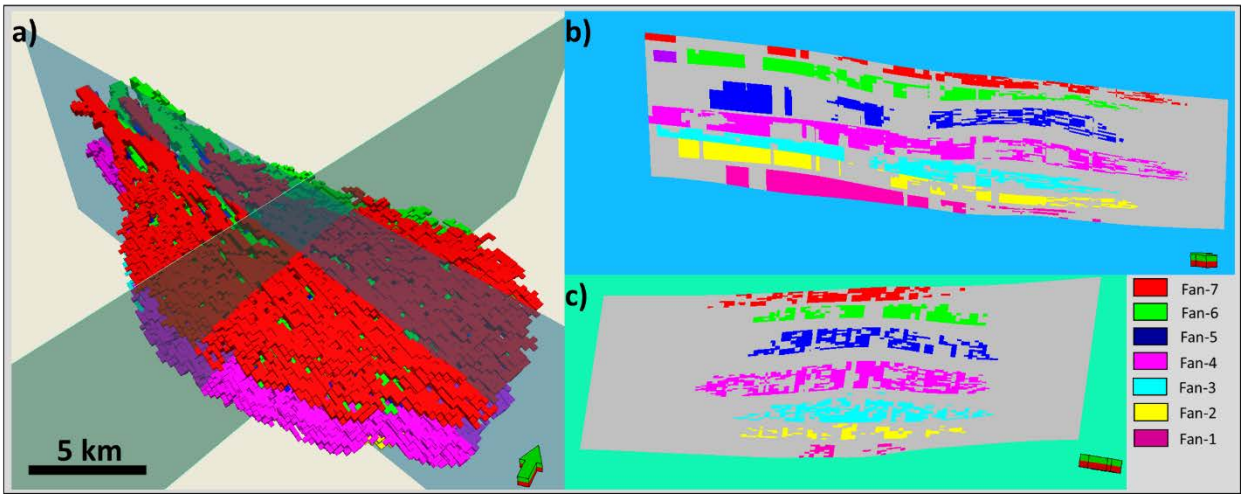

Figure 5-4 The connectivity analysis result for facies model of MPFS method II a) The connected bodies of channel-sand facies and the position of cross-sections b) Cross-section from proximal part to distal part b) Cross-section from central part to marginal part.

5.1.3 MPFS Method III

A group of multilayer training images of three facies is used for this method together with a TGS physical region cube, an azimuth cube and facies probability based on vertical proportion.

This method produces quite a different facies model compared to the facies models of MPFS method I and MPFS method II. The channel of this model is still showing the expected channel thickness change from the proximal to distal part. However, the background-shale facies is cutting the channel especially on top of the fan (Figure 5-5a). The shale facies is randomly distributed showing patches of shale in the central part while it is also dividing each fan as seen in Figure 4-5b. The training image that contains layered sheet-sand is well reproduced showing the shape of sheet. However the distribution of this facies is still disordered and occasionally discontinued from lobe-sand facies as shown in figure 5-5b

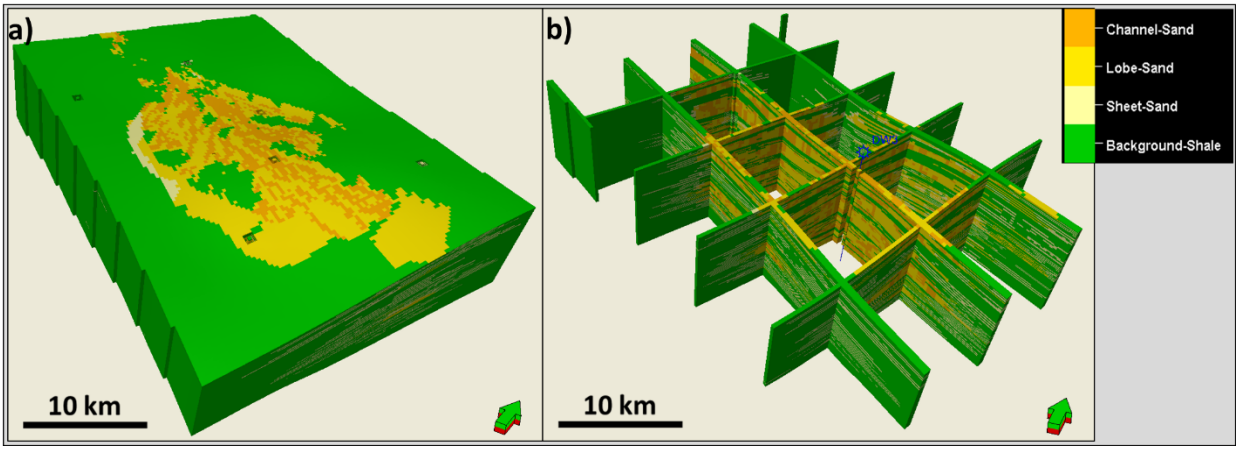

Figure 5-5 The modelling results of third methodology using multilayer of three facies training images a) The facies model showing top of fan-7 b) Cross sections thru the facies model showing its internal architecture.

This model is also having seven massive channel bodies as shown in Figure 5-6a. The transition of the channel thickness is similar to the facies model of MPFS method II. But the channel continuity is less intense compared to the first two methods because the patched shale occurred within the fan (Figure 5-6b and 5-c). In the fan-6, the channel bodies are split into two bodies caused by the shale.

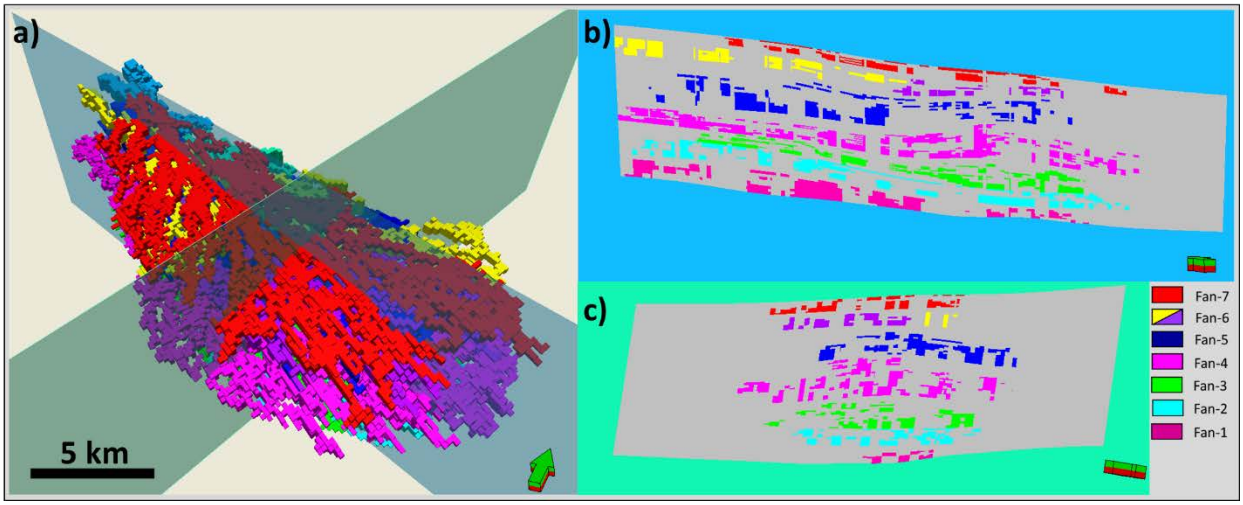

Figure 5-6 The connectivity analysis result of facies model, method 3 a) Connected bodies of channel-sand facies and the position of cross-sections b) Cross-section from proximal part to distal part b) Cross-section from central part to marginal part.

5.1.4 MPFS Method IV

The last method of MPFS is using a group of multilayer training images based on object modelling. For the additional input, this method is also using an edited physical region cube, an azimuth cube, and a facies probability cube based on trend modelling.

The channel width does not change significantly from the proximal part to the distal part of the model compared to three methods discussed above (Figure 5-7a). The lobe-sand and sheet-sand facies have patchy shapes. Figure 5-7b shows the background-shale facies dividing each fan. Sometimes, this facies is also occurred in the middle of central and peripheral part as seen in Figure 5-7b.

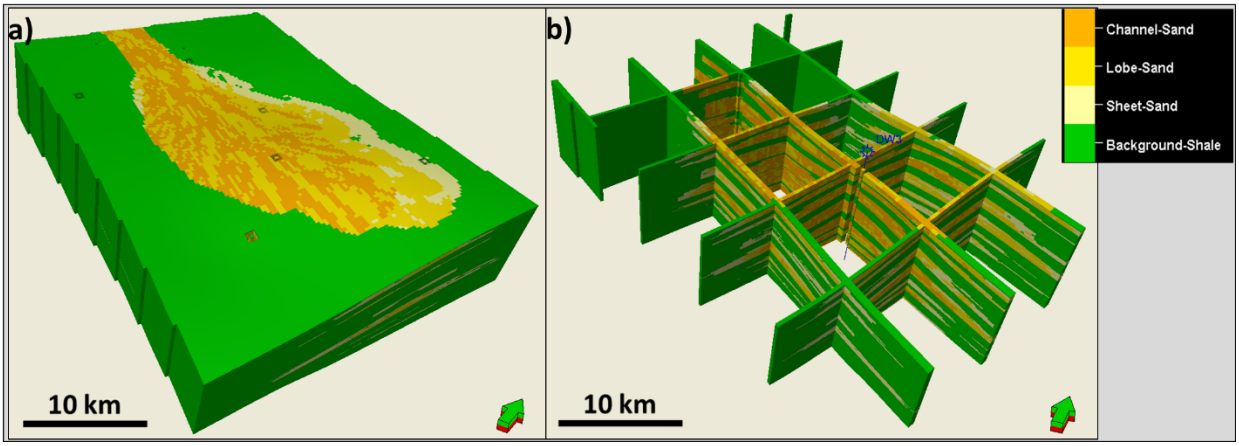

Figure 5-7 The modelling result of MPFS method IV using multilayer object modelling training images a) Facies model showing top of fan-7 b) Cross sections thru the facies model showing its internal architecture.

Figure 4-8a indicates that the continuity of channels is similar to the method I and method II. The changing of channel width also occurs in this model. The channels show a stacked pattern of amalgamated channels as can be seen in Figure 4-8b and 4-8c.

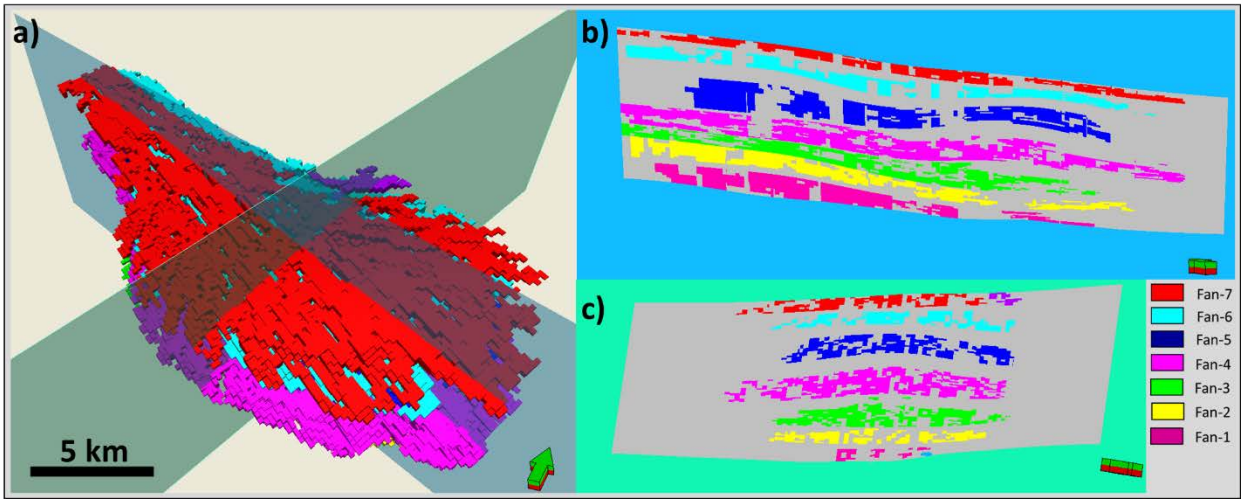

Figure 5-8 The connectivity analysis result of facies model of MPFS method IV a) Connected bodies of channel-sand facies and the position of cross-sections b) Cross-section from proximal part to distal part b) Cross-section from central part to marginal part.

5.2 Gauss Indicator Simulation (GIS)

The GIS method cannot reproduce the geometry of channels as seen in Figure 5-9a which shows the facies model based on this algorithm. The channel-sand facies is modelled as patches whose size is controlled by the variogram parameters. In Figure 5-9b which shows cross sections thru the facies model, the lobe-sand and sheet-sand are well reproduced because they are controlled by the conditioning data using an edited physical region.

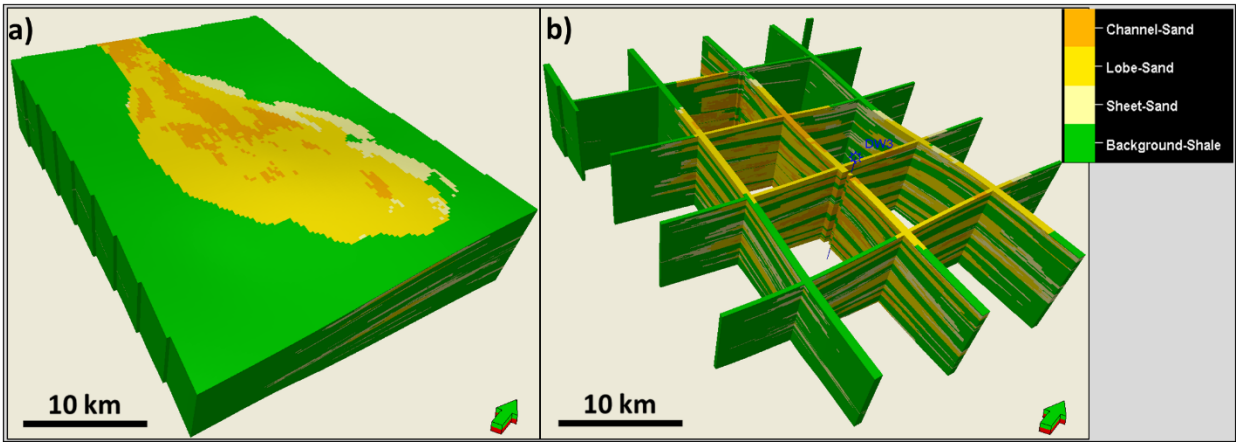

Figure 5-9 The modelling results of pixel-based modelling using Gauss indicator simulation (GIS) a) Facies model showing top of fan-7 b) Cross sections thru the facies model showing its internal architecture.

The distribution and connection of the channel facies of this model is quite different compared to other methods. The channel bodies are separated and distributed in big clusters as shown in Figure

5-10a. The pattern of the channel bodies does not show the typical geometry of channels of a submarine fan system. In cross section view, this model shows the amalgamated channels where the channels in proximal part are thicker than the channels in distal part (Figure 5-10b). But in the central to marginal part, the model shows a poor distribution of the channels. Also the model cannot address the thickness transition as seen in Figure 5-10c. Note that the channel distribution given by GIS is controlled by the 'Seed' number, which is generating the random number used for deriving the facies from the facies probability distribution for each grid cell. This means that a different simulation will result in a different channel sand distribution that may or may not match the conceptual model better.

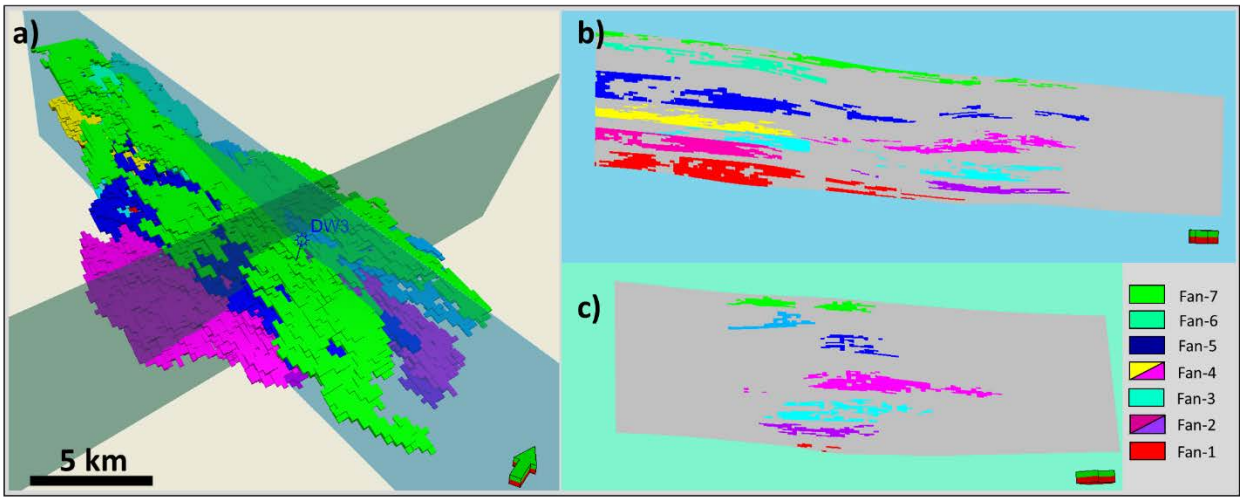

Figure 5-10 The connectivity analysis result of facies model of GIS a) Connected bodies of channel-sand facies and the position of cross-sections b) Cross-section from proximal part to distal part b) Cross-section from central part to marginal part.

5.3 Object Modelling

The facies model of object modelling shows a different result compared to the other methods. The channel distribution is not following the conceptual model. Several channels look like straight continuous sand bands. As can be seen in figure 5-11a, they do not have the distributary character that is expected for channel systems of a submarine fan system. The sheet-sand facies is reproduced as patchy sand and occasionally cut by shale (Figure 5-11b).

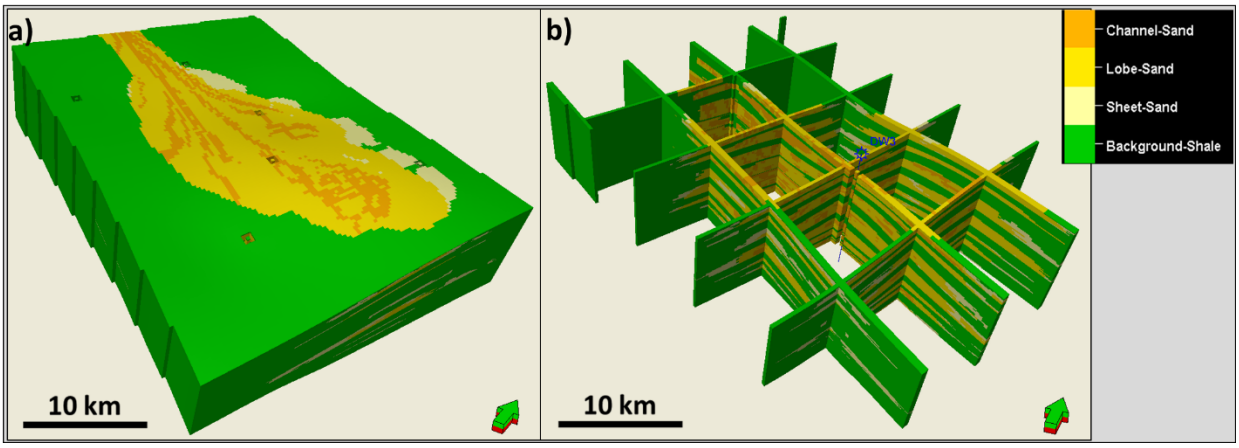

Figure 5-11 The modelling results of object modelling a) Facies model showing top of fan-7 b) Cross sections thru the facies model showing its internal architecture.

The connectivity between the individual channels is poor as can be seen in Figure 5-12a. However the channels are modelled as continuous sand bodies of a length up to 20 km. In Figure 5-12b the channel bodies show lack of connectivity because the individual channels are crossing the cross section. However the cross section from central to marginal part of Figure 5-12c, shows clearly the poor connectivity between the individual channels.

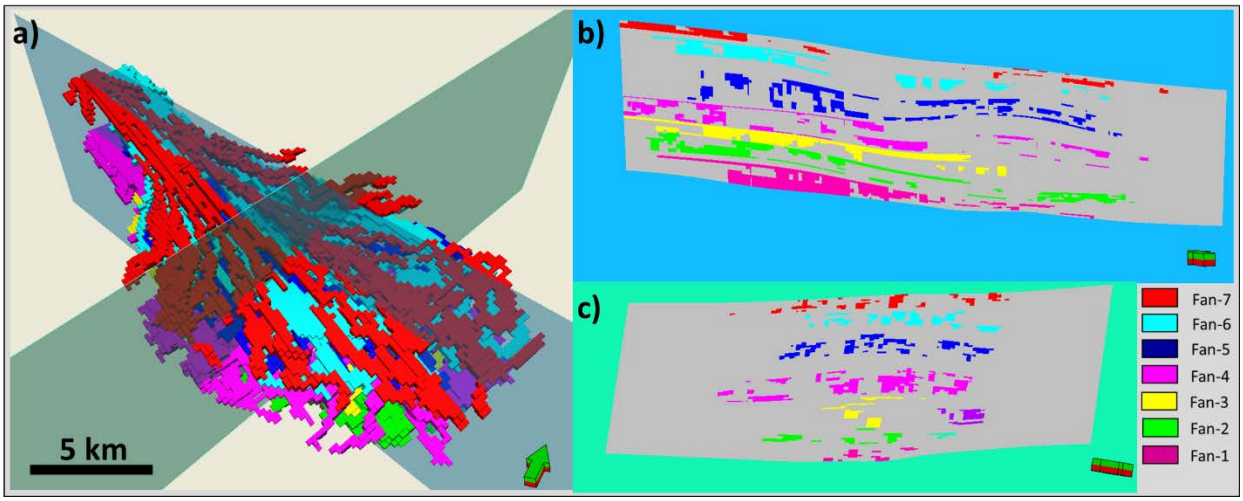

Figure 5-12 The connectivity analysis result for facies model based on object modelling a) Connected bodies of channel-sand facies and the position of cross-sections b) Cross-section from proximal part to distal part b) Cross-section from central part to marginal part

6. DISCUSSION

Multi-point facies simulation (MPFS) is used successfully to reproduce facies models of submarine fan deposits based on different groups of training images. Training images, which are the main drivers of MPFS, play an important role to control the reproduction of facies pattern and geometry. The other important input are:

- The physical modelling region which controls the depositional sub-environment boundaries.
- Azimuth property guiding the local direction of the facies bodies
- Facies probabilities

All these inputs are created based on a conceptual model which is the underpinning of the facies model.

Table 6-1 presents the summary of all facies modelling results. The single layer training images of two facies used by MPFS method I are addressing the channel pattern and honor the stationary condition. However, this training image cannot address changes of facies thickness and is lacking control over the vertical facies distribution. In addition, every zone shows a transitional shale facies at the top. Obviously, neither the shale transition nor the vertical facies changes can be handled by single layer training images of two facies. The shale transition at the fan tops can be addressed thru manually editing the physical region that is mimicking the transition facies. This work can be time consuming and has the additional disadvantage of not being exactly reproducible.

In order to overcome the problem of controlling the vertical facies distribution, a set of multilayer training images of two facies that comprises the architecture of stacked channels is used by the method II of MPFS. This group of training images are similar to the group of single layer training images of two facies in honoring the stationary. However, one still has to work with the edited region to model the shale transition.

MPFS method III tries to simulate the shale transition as well as the channel stack with multilayer training images of three facies: channel-sand, lobe-sand and background-shale. It is clear that this kind of training image is non-stationary and consequently delivers a facies distribution that is partly in conflict with the conceptual model when being used in MPFS. The main problem turns out to be that areas where sand facies should dominate are showing major patches of shale. Using

a modified vertical proportion of the facies as a soft probability improves the simulation result considerably. The advantage of this method is its reproducibility. In addition, the method is very efficient to realize because there is no need for any manual interaction.

An attractive way of setting up multilayer training images is object modelling which is done in MPFS method IV. The calculation of the training images is easily realized because the geometry of the objects can be defined efficiently. However, the vertical distribution of the channel objects is random and may deliver a pattern that is not supported by the conceptual model.

The usage of facies probabilities plays an important role as secondary input to constrain the facies distribution. Strebelle et al. (2010) used a conditioned seismic inversion cube as the facies probability. In this thesis, a facies probability cube is derived from a probability trend model based on the facies logs and a predefined variogram model. However, this method is not optimal to use because of lack of data between the wells.

In order to compare the results of MPFS with other modelling techniques two facies models based on pixel-based modelling and object-based modelling are set up. The edited physical regions of the MPFS method are used as secondary input to constrain the facies distribution. In other words, every region has its own set of parameters i.e. the geometry, shape and facies fraction for object modelling and the variogram models and facies fractions for pixel-based modelling. The azimuth cube is also utilized in both methods to constrain the direction of facies distribution.

The advantage of Gauss indicator simulation (GIS) is its simple setup to follow the probability cubes of the facies. This method is advisable for simple depositional environment such as shoreface deposits. However, the 2-point variogram, which is the base of the GIS algorithm, cannot model the geometry and shape of the facies of submarine fan systems, for example: channel pattern, channel width, sheeted sand etc.

Object modelling allows to create complex facies models. However, the simulation delivers continuous channels crossing the complete modelling region. Such a pattern has a huge impact on the flow simulation. The question is whether this type of channel model can be expected for the study area or else, whether a channel, broken up into a couple of elements is a more realistic representation of the submarine system.

Table 6-1 Summary of facies modelling results.

Method	Map View	Cross Section (Proximal to Distal)	Cross Section (Central to Marginal)
Conceptual Model	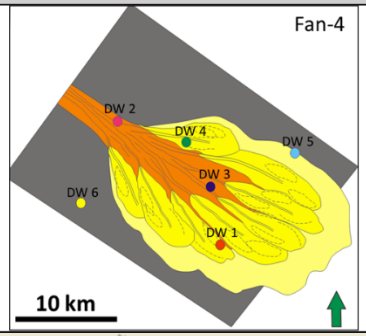	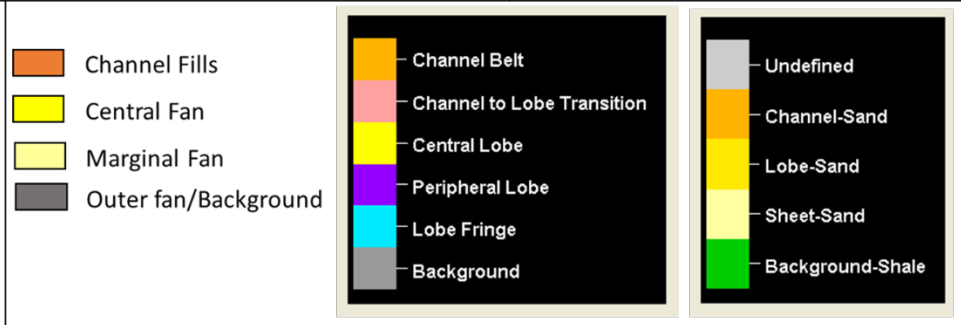	
Edited Physical Region	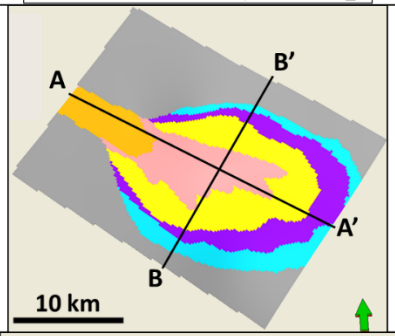	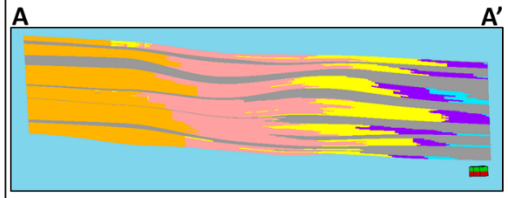	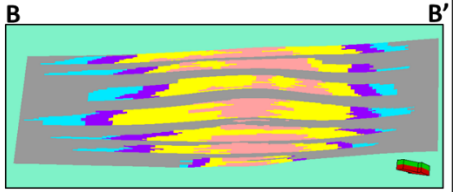
MPFS Method I	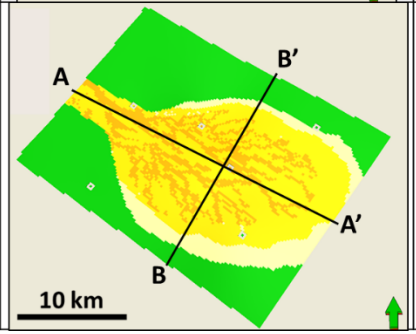	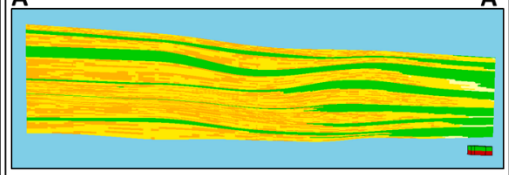	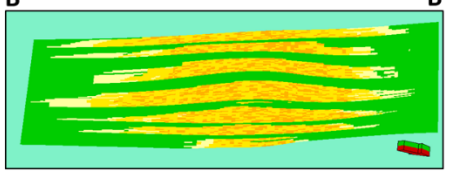

Table 6-1 Continued.

Method	Map View	Cross Section (Proximal to Distal)	Cross Section (Central to Marginal)
MPFS Method II	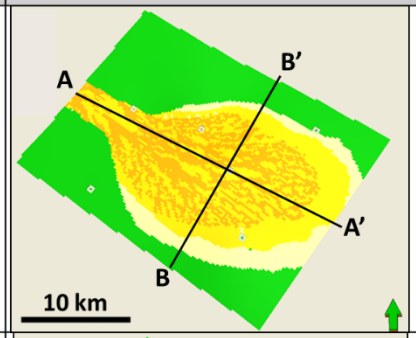	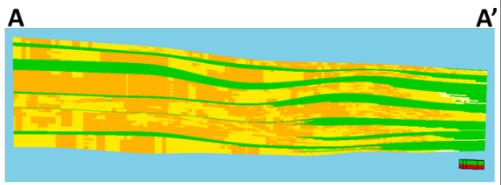	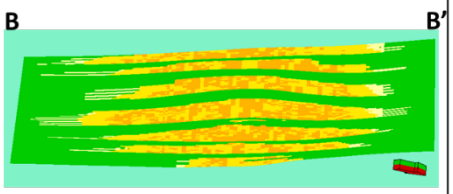
MPFS Method III	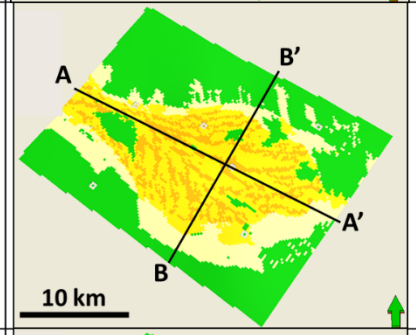	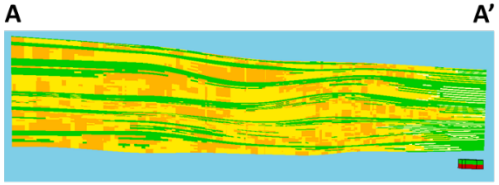	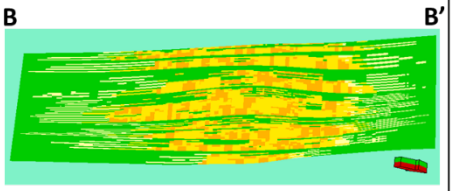
MPFS Method IV	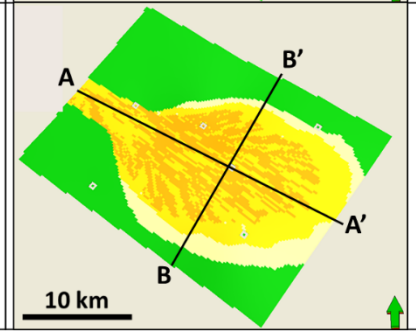	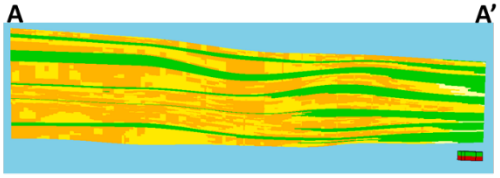	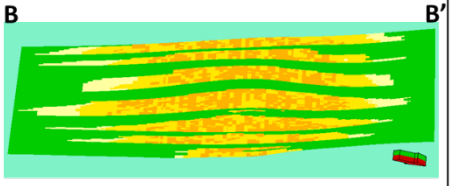

Table 6-1 Continued.

Method	Map View	Cross Section (Proximal to Distal)	Cross Section (Central to Marginal)
GIS	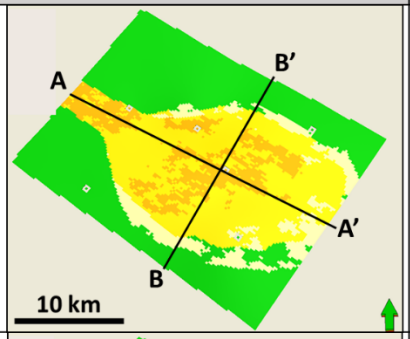	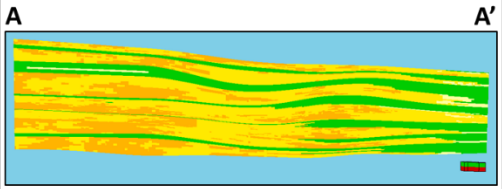	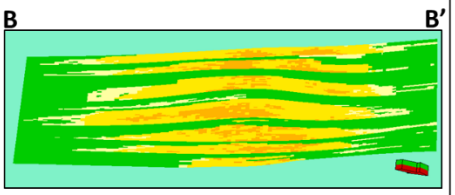
Object Modelling	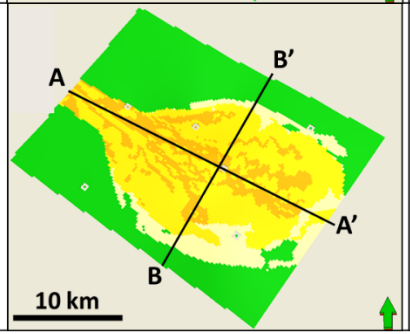	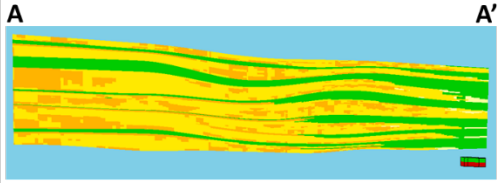	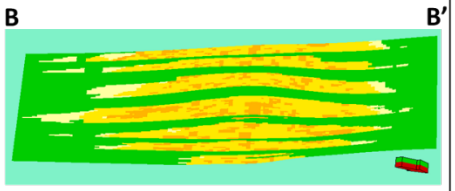

7. CONCLUSION

- Conceptual studies have been successfully used to perform different methods of facies modelling of a submarine fan system.
- A major challenge is the setting up of stationary training images that reflect the facies body size in all three dimensions properly.
- Stacked channels can be better reproduced by using multilayer training image compared to a single layer training image.
- This study shows that the difficulty in simulating realistic facies models is manageable when subdividing the study area into regions guided by the changes of the depositional environment.
- Capturing the vertical distribution of facies thru multilayer training images remains a major challenge which can be addressed (at least partly) by the usage of vertical probability functions.
- Pixel-based facies modelling is a very efficient method suited for simple depositional environments. Obviously this technique is not suitable for modelling facies bodies.
- The object-based facies method allows to easily and efficiently model several types of facies bodies. Although it does not provide the modelling flexibility of MPFS it allows to set up complex depositional environments.
- Facies modelling based on MPFS has been proven to be a flexible and powerful method for modelling complex depositional environments, i.e. submarine fan, alluvial fan, delta and estuary. However this modelling tool is not easy to handle and the user needs some experience in order to build reliable facies models.
- All three modelling techniques are honoring the input facies fractions. Consequently, applied to the same depositional environment, all three techniques will deliver similar reservoir volumes.

- However, and this is a major differentiator between the three discussed techniques, the three modelling methods deliver sand bodies that show large differences in their internal connectivity. For instance the channels of object modelling are very extended and continuous sand bodies. The channels of MPFS may be broken up delivering less connectivity. Gauss indicator simulation delivers sand patches of the size controlled by the variogram ranges. Consequently the connected sand bodies are much more heterogeneous compared to, for instance, the channels of object modelling.
- The connectivity of the sand bodies has a huge impact on the permeability distribution and consequently on the performance of the wells.
- Resources, especially time needed for model setup and model calculation, should be considered before choosing the facies modelling technique because not all reservoirs need advanced facies modelling technique.
- The facies modelling technique needs to be carefully chosen because of its impact on the flow behavior. Consequently the modelling technique should be discussed with the reservoir engineer.

8. FUTURE WORK

This thesis has outlined methodologies and best practices of multi-point facies simulation (MPFS). For future research, an uncertainty analysis should be carried out to investigate which MPFS parameters have a major influence on the reservoir volume uncertainty. Also, in order to better understand and compare the flow behavior of alternative models, flow line simulations should be effectuated. This simple simulation technique is also recommended for estimating the P10, P50 and P90 reservoir volumes of the reservoir models derived from facies and reservoir property simulations.

9. REFERENCES

Arpat, G. B., 2005. Stochastic simulation with patterns: doctoral dissertation, Stanford University, Stanford, USA, 184 p.

Arpat, G. B., & Caers, J. (2007). Conditional Simulation with Patterns. Mathematical Geology, 39(2), 177-203. doi: 10.1007/s11004-006-9075-3

Fielding, C. R., & Crane, R. C. (1987). An Application of Statistical Modelling to the Prediction of Hydrocarbon Recovery Factors in Fluvial Reservoir Sequences. Recent Developments in Fluvial Sedimentology: The Society of Economic Paleontologists and Mineralogists (SEPM) Special Publication 39, 321-327.

Guardiano, F. B., & Srivastava, R. M. (1993). Multivariate Geostatistics: Beyond Bivariate Moments. In A. Soares (Ed.), Geostatistics Tróia '92: Volume 1 (pp. 133-144). Dordrecht: Springer Netherlands.

Harris, P. M., Kenter, J., Playton, T., Andres, M., Jones, G., & Levy, M. (2011). Enhancing Subsurface Reservoir Models – An Integrated MPS Approach Using Outcrop Analogs, Modern Analogs, and Forward Stratigraphic Models. Search and Discovery Article #50419 (2011), AAPG Annual Convention and Exhibition, Houston, Texas, USA, April 10-13, 2011.

Journel, A. G. (1994). Geostatistic and Reservoir Geology. Stochastic Modelling and Geostatistics Principles, Methods, and Case Studies, AAPG Computer Applications in Geology, No. 3, 2.

Nichols, G. (2009). Sedimentology and Stratigraphy (2nd Edition). Hoboken: Hoboken, NJ, USA: Wiley-Blackwell.

Piper, D., & Normark, W. (2009). Processes That Initiate Turbidity Currents and Their Influence on Turbidites: A Marine Geology Perspective J. Sediment. Res. (Vol. 79, pp. 347-362).

Ravnås, R., Cook, A., Engenes, K., Germs, H., Grecula, M., Haga, J., Harvey, C., Maceachern, J. A. (2014). The Ormen Lange turbidite systems: sedimentary architectures and sequence structure of sandy slope fans in a sediment-starved basin. International Association Sedimentology Special Publication, 46, 38.

Reading, H. G., & Richards, M. (1994). Turbidite systems in deep-water basin margins classified by grain size and feeder system. AAPG Bulletin, 78, 792-822.

Strébelle, S., Geological, S. U. D. o., & Sciences, E. (2000). Sequential Simulation Drawing Structures from Training Images: Stanford University.

Strebelle, S., Payrazyan, K., & Caers, J. (2003). Modelling of a deepwater turbidite reservoir conditional to seismic data using principal component analysis and multiple-point geostatistics. Spe Journal, 8(3), 227-235.

Tetzlaff, D., Davies, R., McCormick, D., Signer, C., Mirowski, P., & Williams, N. (2005). Application of multipoint geostatistics to honor multiple attribute constraints applied to a deepwater outcrop analog, Tanqua Karoo Basin, South Africa. SEG Technical Program Expanded Abstracts 2005, 1370-1373. doi: doi: 10.1190/1.2147942

Zhang, T. (2009). Introduction to MPS and a Guide to Using Multi-point Facies Modelling in Petrel 2009.1Schlumberger-Doll Research (Vol. 1, pp. 60).